Chapter 19

Seismic Vibration Sensor with Acoustic Surface Wave

Jerzy Filipiak and Grzegorz Steczko

Additional information is available at the end of the chapter

http://dx.doi.org/10.5772/55445

1. Introduction

Mechanical vibrations are a movement of particles around the state of equilibrium in a solid environment. Vibrations are a common phenomenon in our daily life. These vibrations are often parasite effects threatening our existence. Vibrations of the ground, machines, or a number of technical devices present a process, which require a continuous or a long-term monitoring. In many sectors vibrations are a working factor in a production process.

Mechanical vibrations serve as a source of information in medicine, diagnostics of the structure of many machines and in perimeter protection (monitoring). The knowledge of vibration parameters allows evaluating the technical condition of machines, the quality of their design and manufacture and their reliability. Early detection of ground vibrations serves to predict and warn of earthquakes. Ground vibrations serve to monitor explosions and are used in the reflexive seismology (prospecting for mineral deposits). Detection of ground vibrations in systems of perimeter protection allows detecting an intrusion into an area under surveillance. Mechanical vibrations are characteristic for their differing frequencies and amplitude. The frequency of mechanical vibrations ranges usually from a hundredth of Hz to a dozen or so kHz. Parameters of mechanical vibrations are measured with vibration sensors.

At present practically three types of seismic sensors are used:

- geophones,
- piezoelectric acceleration sensors,
- micro-mechanical silicone acceleration sensors.

Geophones belong to the simplest and most inexpensive vibration sensors. They feature a low mechanical resonance frequency, which ranges usually between 4Hz and 14Hz. They

are used in mining, for safety perimeter protection [1] and in the reflexive seismology (Figure 1).

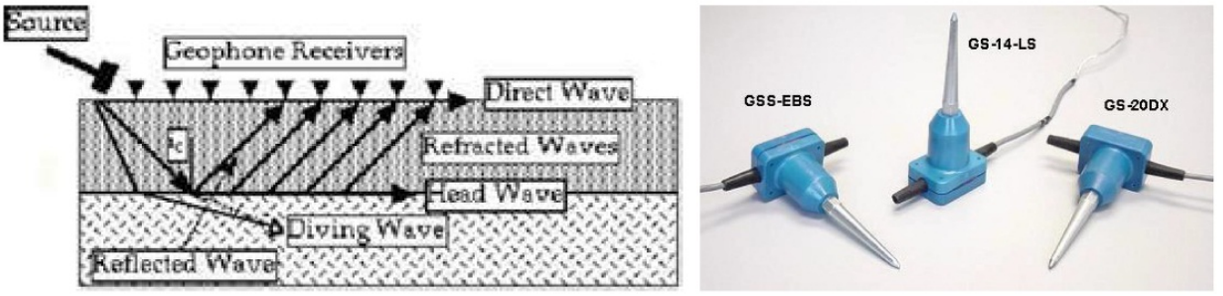

Figure 1. Reflexive seismology and geophones [1]

Micro mechanical silicone acceleration sensors (MEMS) [2-3] are mass-produced and used in many fields (e.g. deploying air bags, laptops). They are characterised by small dimensions. Due to their miniature dimensions their mechanical resonance frequency is very high, usually a dozen or so kHz or a few dozen kHz. With piezoelectric acceleration sensors [4] one can measure variable accelerations. Their mechanical resonance frequency is higher than that of MEMS.

Figure 2. Seismometers offered by MEROZET 1 - portable broadband seismometer, 2 - very broadband seismometer 3 - triaxal seismic accelerometer.

Figure 2 shows seismometers offered by MEROZET: a portable one, a wide-band and a triaxial one; all these 3 models are based on and include piezoelectric acceleration sensors. Vibration sensors can be built using sensors with the acoustic surface wave (SAW).

These SAW-based sensors are used to measure a number of physical quantities: gas concentration [5-8], temperature, pressure [9-13], and mechanical quantities: torque of a rotating shaft [14], stress [15-17], acceleration [18-19] and vibrations [20-21]. All these SAW–based sensors work on the basis of measuring changes in the delay of a surface wave due to the impact of a physical quantity being measured on its speed and the propagation path. However, depending on the kind of a measured physical quantity, a number of problems occur, which are characteristic for the group of sensors used for measuring that quantity.

Figure 3. Basic structure of a SAW vibration sensor

Figure 3 presents the idea of the structure of an SAW-based sensor. The main element of this sensor is an anisotropic plate of a piesoelectric material. One end of the piesoelectric plate is made fast to the sensor housing, while on the other free end a seismic mass can be placed. An SAW-delaying line in the form of a four-terminal-network is made on the top surface of the sensor. The movement of the sensor housing causes its plate to vibrate and the SAW-based delaying line delay to change. This is why the phase of a high frequency signal passing thru such a line changes. The magnitude of a signal pahse change will be proportional to the change in the delay of an SAW-based delaying line.

The presented sensor design presents three different issues, which must be solved:

- modeling of the sensor mechanical system, which amounts to the description of plate deformations and stresses occurring in it.
- modeling of the sensor mechanical-electrical converter – delaying line with the SAW, which amounts to the description of the change in parameters of a delaying line with the SAW (first of all of the delay) due to distortions and stresses in the plate
- modeling of the electric circuit cooperating with the sensor, which amounts to the analysis and synthesis of an electric circuit measuring the changes in the delay of the surface wave in a delaying line including the SAW.

The work presents a solution of the mentioned problems, which were further analysed. The work presents executed models of SAW-comprising sensors and the results of a study of their parameters. The use of realised sensors in a system of perimeter protection is described. The structure of an SAW-comprising sensor (Fig. 3) is a combination of a continous system in the form of a piesoelectric, anisotropic support plate and a discrete system in the form of a concentrated mass. In theory such a system can feature an infinite number of free vibration frequencies. Writing a description of the mechanics of the plate of an SAW-based vibration sensor is a complicated proces; what makes it dificult is the tensor description of the plate mechanical properties. The knowledge of the value of an attenuation tensor (viscosity tensor) poses a problem. Therefore an analysis was conducted, which allows to simplify the sensor model presented in Figure 3 and next as a result of this analysis the movement of a piesoelectric, anisotropic plate with a concentrated mass was described with the aid of a discrete system of one degree of freedom. Elastic and viscous properties of the plate material were taken into account. This model was introduced by way of an isotropic descritpion of anisotropic material properties. The model accuracy was evaluated. Explicit realtionships between sensor plate movement parameters and its geometey and parameters describing its elastic an viscous properties were determined, thus

a simple analysis and synthesis of the sensor plate movements were possible. The main feature of the sensor mechanical system (a continous system combined with a discrete one) is the occurence of pratically only one resonance frequency. A simple description of this magnitude by design parameters of the system and elastic and viscous plate parameters allow a simple modelling, how these sensors function, and as well to determine elastic and viscous parameters of a plate empirically. These parameters in the form : an equivalent Young's modulus and an equivalent material damping coefficient for a selected direction of a piezoelctric substrate (i.e. the direction of the surface wave propagation) were determined in works [22][23]. In available bibliography they are not knowen or utilised. The above considerations are presented in the work [21]. For a full description of the SAW-comprising vibaration sensor designing process in Section 2 we present a modelling process of its mechanical system.

2. Model of mechanical unit for SAW vibration sensor

The object of consideration has been presented in Figure 4. One end of the plate is stiffly attached, and the other is free and without any concentrated mass. The piezoelectric properties of sensor plate will be omitted in the analysis.

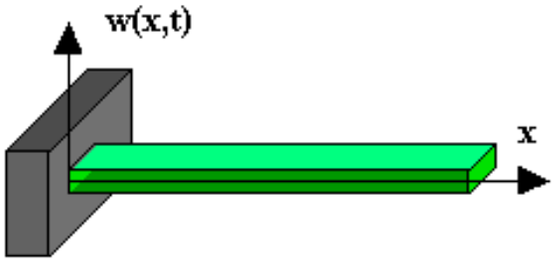

Figure 4. The plate of a vibration sensor.

The equation of a movement of an anisotropic body with the mass density ϱ is:

$$\frac{\partial \sigma_{ij}}{\partial x_j} + \rho \frac{\partial^2 u_i}{\partial t^2} = 0 \tag{1}$$

The stress tensor σ_{ij} depends on the strain tensor ε_{kl} through Hook-Voight equation:

$$\sigma_{ij} = C_{ijkl}\varepsilon_{kl} + \Sigma_{ijkl}\varepsilon_{kl,t} \tag{2}$$

where: C_{ijkl}—is a elasticity tensor, Σ_{ijkl}—is a material damping tensor, u_i—is a displacement vector,

$$\varepsilon_{kl} = \frac{1}{2}\left(\frac{\partial u_k}{\partial x_l} + \frac{\partial u_l}{\partial x_k}\right) \quad - \text{ is a strain tensor} \tag{3}$$

The mathematical description of this issue will be closed if the initial and boundary conditions are added to the aforementioned equations. It is complicated to solve the

problem. The causes of the complications are huge number of non-vanishing modules of an elasticity and material damping tensor. The material damping tensor Σ_{ijkl} has an identical symmetry as the elasticity tensor C_{ijkl}. For materials used in SAW devices (quartz, lithium niobate), the value of damping constants are difficult to experimental verification. For higher class of symmetry of an anisotropic materials, equations (2, 3) are simple. For the isotropic material the elasticity tensor has only two independent components $C_{1111}=\lambda+2\mu$, $C_{1122}=\lambda$, $C_{2323}=\mu$. Therefore the elastic properties of an isotropic substance describe two quantities (λ, μ). They are often shown in form of a Young's modulus E and a Poisson ratio ν. The following relations occur between quantities E, ν, and elasticity tensor components [24]:

$$E = c_{2323}\left(2 + \frac{c_{1122}}{c_{1122} + c_{2323}}\right), \quad \nu = \frac{c_{1122}}{2\left(c_{1122} + c_{2323}\right)} \tag{4}$$

The description of viscous properties of an isotropic body done by material damping tensor is analogical. It is usually described by two quantities [24]:

$$\tau = \frac{\Sigma_{2323}}{E}\left(2 + \frac{\Sigma_{1122}}{\Sigma_{1122} + \Sigma_{2323}}\right), \quad \eta = \frac{\Sigma_{1122}}{2\left(\Sigma_{1122} + \Sigma_{2323}\right)} \tag{5}$$

The Young's modulus E is described as a proportion of a longitudinal stress to longitudinal strain for the direction of the functioning of a stress. To describe the mechanical properties of anisotropic materials taking into account a particular direction of the stress an effective Young's modulus may be used E [24][25](Its magnitude is described by overt dependence). An exemplary expression for a inverse effective Young's modulus for a trigonal unit (lithium niobate, quartz) is:

$$1/E = (1-l_3^2)^2 s_{11} + l_3^4 s_{33} + l_3^2(1-l_3^2)(2s_{13} + s_{44}) + 2l_2 l_3 (3l_1^2 - l_2^2) s_{14} \tag{6}$$

where: s_{ij}—is an element of an compliance matrix, l_j—is a cosine of an angle between the chosen direction and the axis − j, in Cartesian coordinates. The compliance matrix s_{ij} is reverse to the stiffness elasticity matrix c_{ij}.

It is possible to calculate the values of material damping coefficients in a chosen crystallographic direction, too. The presented approach allows to model the anisotropic material by the isotropic model. In a such model the stresses are the sum of elastic and dissipative components:

$$\sigma = E\varepsilon + E\tau\frac{\partial \varepsilon}{\partial t} \tag{7}$$

We consider equivalent isotropic model of cylindrically bent plate [19]. Equation of free vibrations has the form:

$$\rho \frac{\partial^2 w(x,t)}{\partial t^2} + E_e \frac{h^2}{12}\left(1 + \tau \frac{\partial}{\partial t}\right)\frac{\partial^4 w(x,t)}{\partial x^4} = 0 \tag{8}$$

where: ρ—mass density, h—plate thickness, L—plate length, τ—equivalent material damping coefficient , $E_e = \dfrac{E}{1-\nu^2}$

E_e is an equivalent Young's modulus.

At the boundaries we have:

$$w(0,t) = 0, \quad \frac{\partial w(0,t)}{\partial x} = 0, \quad \frac{\partial^2 w(L,t)}{\partial x^2} = 0, \quad \frac{\partial^3 w(L,t)}{\partial x^3} = 0, \tag{9}$$

The solution to the boundary problem (8), (9) has the form:

$$w(x,t) = \sum_{n=1}^{\infty} W_n(x) \cdot A_n \cdot e^{-\frac{\varpi_n^2}{2}t} \cdot \sin(\bar{\omega}_n t + \varphi_n) \tag{10}$$

where: constants A_n and ϕ_n are determined by initial conditions.

The angular frequency of non-damped vibrations is equal to:

$$\omega_n = k_n^2 \frac{h}{l^2}\sqrt{\frac{E_e}{12\rho}} \ . \tag{11}$$

The angular frequency of damped vibrations is equal to:

$$\bar{\omega}_m = \omega_m \sqrt{1 - \frac{\omega_m^2 \tau^2}{4}} \tag{12}$$

$$\text{where}: \mathrm{k}_1 = 1{,}875, \ \mathrm{k}_2 = 4{,}694, \ \mathrm{k}_3 = 7{,}855 \tag{13}$$

The orthonormal set of function W_n (eigenfunctions) is taken from [26]. Only some elements in the sum (10) represent vibrations. For $N < n$ where N is the greatest natural number for chich $\omega_n < 2/\tau$, the element of sum represents very strongly dumped movement and there is no resonance at this frequency. Each of the harmonics n=1,2,3… has part of energy. How great is the part depends on the unit (normal vibrations, ω_n, $w(x)$) and depends on activation. In the paper [18][19][27][28] a simplified model with one degree of freedom was presented and it is shown in Figure 5. It has been used to describe the dynamics of sensor plate movement. It was derived according to the Rayleigh method. This method is based on a simplified modeling of a plate with the use of an equivalent circuit with one degree of freedom which is energetically equivalent. The free end of sensor plate has been taken as a point of reduction. The equivalent circuit present Figure 5

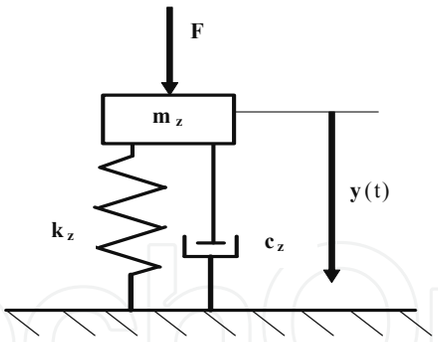

Figure 5. The equivalent circuit of sensor plate with one degree of freedom.

Parameters in the model are as follows [18]:

$$m_z = 0.25196\,\rho b h l, \quad k_z = 3.1169\frac{E_e\, b\, h^3}{l^3}, \quad c_z = \tau\ 3.1169\frac{E_e\, b h^3}{l^3} \tag{14}$$

where: b — plate width

The model with one degree of freedom has only one resonance frequency. The equation of mass movement is as follows:

$$\frac{d^2y(t)}{dt^2} + \omega_0^2\tau\frac{dy(t)}{dt} + \omega_0^2 y(t) = \frac{F(t)}{m_z}\,. \tag{15}$$

The solution of an equation for natural vibrations:

$$y(t) = Ae^{-\frac{\omega_0^2\tau}{2}t}\sin(\omega_r t + \phi)\,, \tag{16}$$

where:

$$\omega_0 = 3.5172\left(\frac{h}{l^2}\right)\sqrt{\frac{E_e}{12\,\rho}}\,, \tag{17}$$

$$\omega_r = \omega_0\sqrt{1 - \frac{\omega_0^2\tau^2}{4}} \tag{18}$$

It is analogical to the Equation (10) obtained with the use of an isotropic model of sensor plate. Comparison of the first frequency of damped vibrations of the plate obtained in an isotropic model (11) and the frequency of damped vibrations obtained with the use of a model with one degree of freedom (17) are in fulfils relation:

$$\omega_1 = 0.9996\omega_r\,, \tag{19}$$

First frequency of damped vibrations calculated in an isotropic model is 0.5 per cent lower than frequency calculated with the use of a discrete model. This difference could be smaller

in case of a sensor construction with the concentrated mass attached to the movable end of the plate. That is why the model with one degree of freedom may be used to describe the movement of sensor plate. It allows relatively easy simulation of vibrations of the plate with the mass attached to its movable end. Free vibrations of sensor plate are a definite as a sum of damped harmonic frequency vibrations. But, in free vibration damped vibrations with first harmonic frequency will dominate. The amplitudes of the superior harmonic vibrations will be extremely small. As it is shown in [18] their quantity is 40 dB smaller than the first harmonic amplitude. This is the reason why a model with one degree of freedom [18][27][28] has been used to analyze the movement of the plate with concentrated mass. Vibrations of the plate have been activated by the movement of the sensor casing *Y(t)*. The equation of movement is as following:

$$\frac{d^2y(t)}{dt^2} + \omega_0^2\tau\frac{dy(t)}{dt} + \omega_0^2 y(t) = \omega_0^2\tau\frac{dY(t)}{dt} + \omega_0^2 Y(t)\ . \tag{20}$$

where:

$$\omega_0 = 3.5172\left(\frac{h}{l^2}\right)\sqrt{\frac{E_e}{12\,\rho}}\sqrt{\frac{1}{1+r\ 3.9689}} \tag{21}$$

r is a ratio between seismic mass and mass of sensor plate.

The solution of the Equation (20) is a function:

$$\begin{aligned} y(t) &= A\exp\left[-\frac{\omega_0^2\tau t}{2}\right]\sin\left[\omega_r(t+\varphi)\right] - \\ &-\frac{4\omega}{4-\omega_0^2\tau^2}\int_0^t\left(\tau\frac{dY(\xi)}{dt} + Y(\xi)\right)\cdot\exp\left[-\frac{\omega_0^2\tau}{2}(t-\xi)\right]\cdot\sin\left[\omega_r(t-\xi)\right]d\xi \end{aligned} \tag{22}$$

where: constants A and φ are determined by initial conditions.

Relations between ω_0 and ω_r are as in identity (18). In both components of the solution (22) appears the following function:

$$\varphi_\delta(t) = Ae^{-\frac{\omega_0^2\tau}{2}t}\sin(\omega_r t + \phi) \tag{23}$$

It is a product of a harmonic and damping (exponentially decay with time) function. The frequency of a harmonic function is the resonance frequency of the unit. This function describes sensor impulse response and its natural vibrations. It is a sum of:

- convolution of an impulse response of the plate and the component of describing movement of the sensor casing,
- damped vibrations with the resonance frequency of a sensor plate.

It will always have a factor in form of a harmonic function with the frequency equal to the resonance frequency of sensor plate and with variable amplitude. That is why the frequency response of sensor plate may be quantity identifying the sensor. Frequency response of the sensor plate is the ratio of the amplitude of the deflection plate sensor to the harmonic amplitude of its case The frequency response of the sensor plate calculated from the Equation (20) is as follow:

$$H(\omega) = \sqrt{\frac{1+(\omega\tau)^2}{[1-(\frac{\omega}{\omega_r})^2]^2+(\omega\tau)^2}} \tag{24}$$

Parameters in relation (24) depends on mechanical properties of the sensor plate material. The quantities of elastic and viscous parameters for quartz are shown in Table 1 [22][23].

	ST-cut quartz
Equivalent Young's modulus [GPa]	76
Dynamic critical compressive stress [MPa]	80
Equivalent material damping coefficient [μs]	29.3
Density [kg/m^3]	2650

Table 1. Material parameters of quartz.

Theoretical frequency response for plates made of ST-cut quartz with the resonance frequencies of 22 Hz and 100 Hz are shown in Figure 6. The most important is that for low frequency the frequency response has narrower band and higher magnitude so the selectivity of the sensor is high. It decreases with increased resonance frequency.

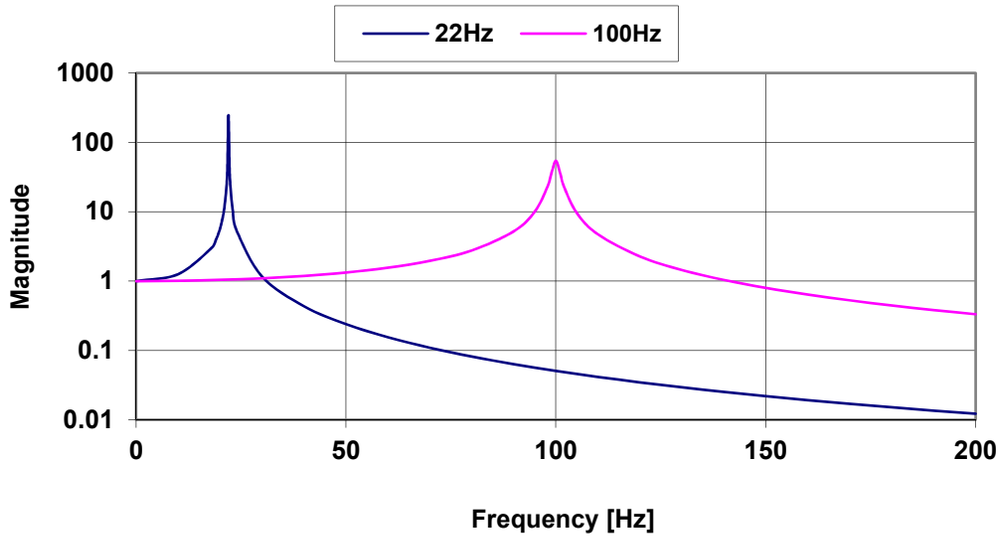

Figure 6. Theoretical resonance characteristics of plates with resonance frequencies of 22 Hz and 100 Hz.

The maximum value of the frequency response of the plate will occur for $\omega = \omega_r$. It has been described with the relationship:

$$H(\omega_r) = \sqrt{\frac{1+(\omega_r \tau)^2}{(0,5\omega_0 \tau)^4 + (\omega_r \tau)^2}} \tag{25}$$

Its value exceeds repeatedly the value of static deflection. (e.g., for the resonance frequency of 22 Hz it is 246 times higher).

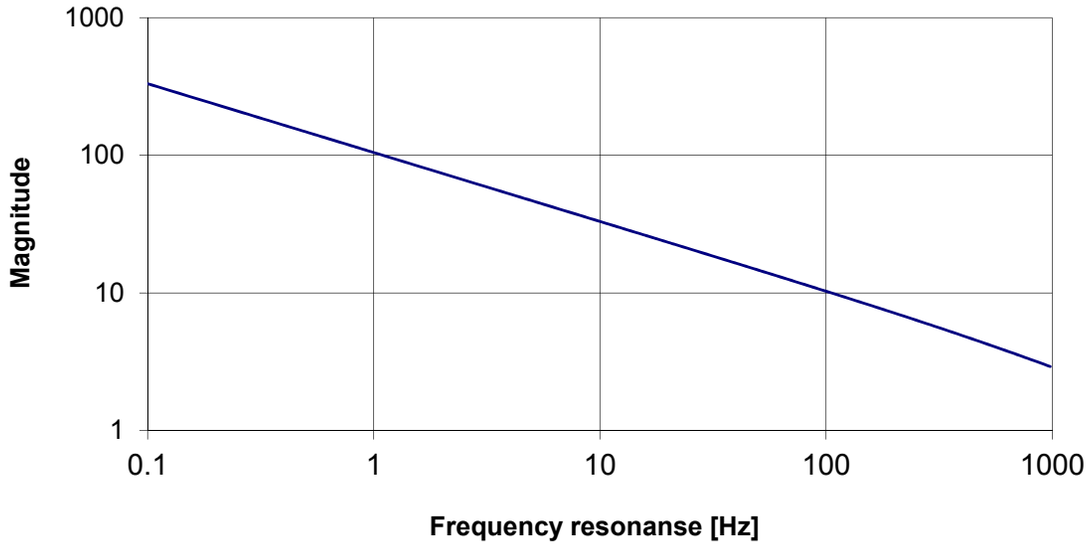

Figure 7. Maximum magnitude of frequency response versus the resonance frequency of the sensor plate.

The change in maximum magnitude of frequency response as a function of resonance frequency of the plate is shown in Figure 7 For the resonance frequency of a plate of 10Hz the vibrations amplitude multiplication is 1,600 higher than static deflection. This property may be used to construct sensors with high sensitivity level. But it is necessary to answer one question beforehand: what is the lowest possible resonance frequency of a plate that we can manufacture? The answer is accessible on the basis of the described model and the length of available plates. The resonance frequency of sensor plate is described by the relation (21). It depends on plate length (l) and on quantity of a concentrated mass (r) attached to the free end of sensor plate. The increase of the concentrated mass lowers resonance frequency of the plate, simultaneously increasing stresses of the plate.

The influence of a change of concentrated mass on resonance frequency of the sensor plate is shown in Figure 8.

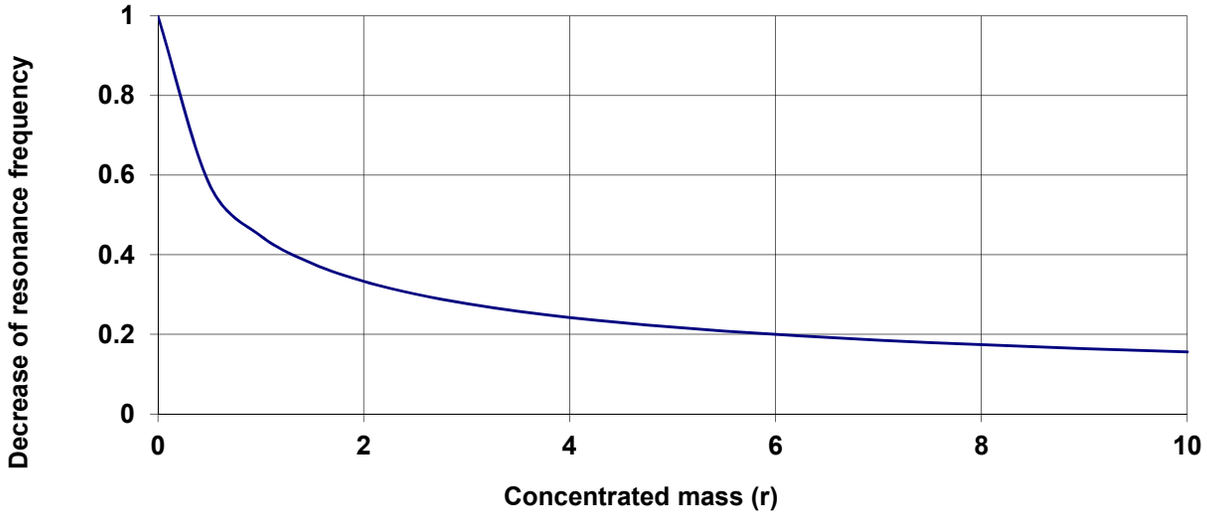

Figure 8. The influence of a change of a concentrated mass on sensor plate resonance frequency.

It is visible that the use of concentrated mass quantities exceeding two times the mass of the plate enables and triple decrease of resonance frequency of a plate. It is the most effective place to decrease the resonance frequency of a plate. Continuous increase of a concentrated mass does not substantially decrease the resonance frequency of sensor plate. The further analysis of sensor parameters will be limited to such range of concentrated mass quantities. The relationship between the value of resonance frequency of a plate made of ST-cut quartz and length of the plate determined by three different concentrated mass values is shown in Figure 9.

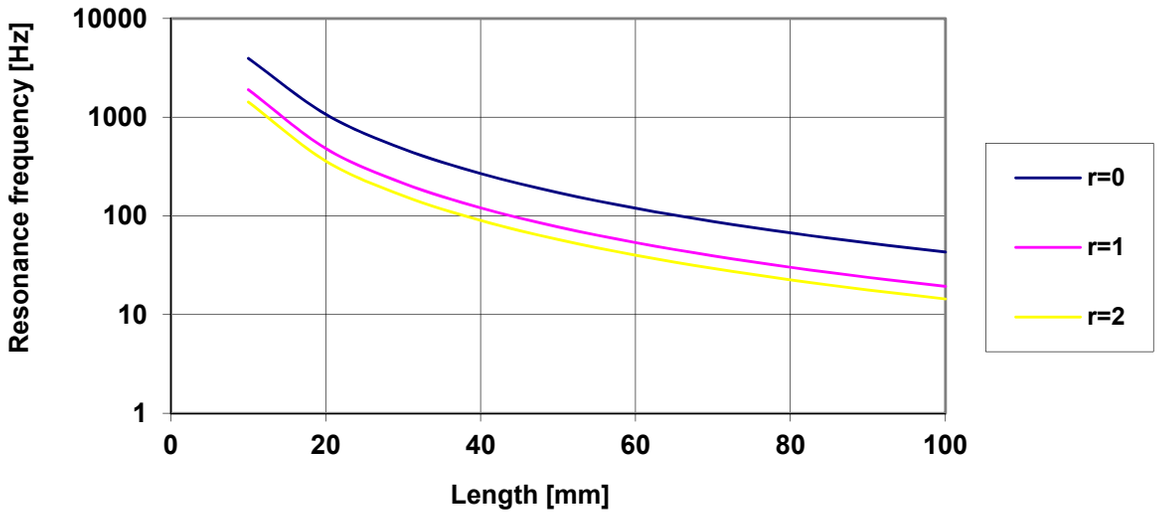

Figure 9. The relationship between sensor plate resonance frequency made of ST-cut quartz 0.5 mm thick, and plate length (l) and the quantity of concentrated mass (r).

From the figure presented above may conclude that it is relatively easy to create plates of resonance frequency form 20 Hz do 4 kHz. For the 0.5 mm thick plates it is necessary to use the concentrated mass up to 1.5 g. The relation between the concentrated mass and the plate length is shown in Figure 10. The sensor impulse response presented by the relation (23) has a damped character. Its fast fading can impose an upper limit of the resonance frequency. The damping value depends on the geometry of the plate and the equivalent damping coefficient. In order to simplify the illustration the impulse response damping measure has been introduced as a relative decrease of its quantity after one period.

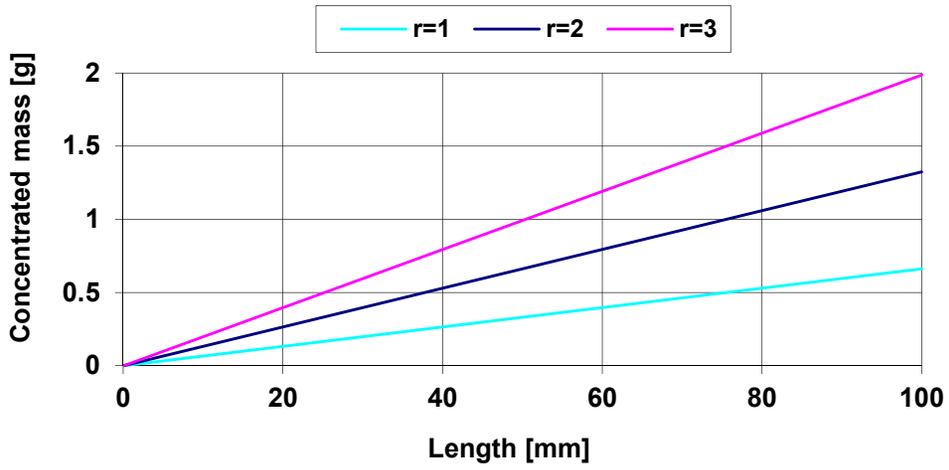

Figure 10. The concentrated mass quantities used in the considered sensor constructions.

The relation of impulse response damping in form of a function of length of ST-cut quartz plate for three different concentrated mass values is presented in Figure 11. For plates longer than 40 mm loaded by the concentrated mass equal to the mass of the plate (r = l) the

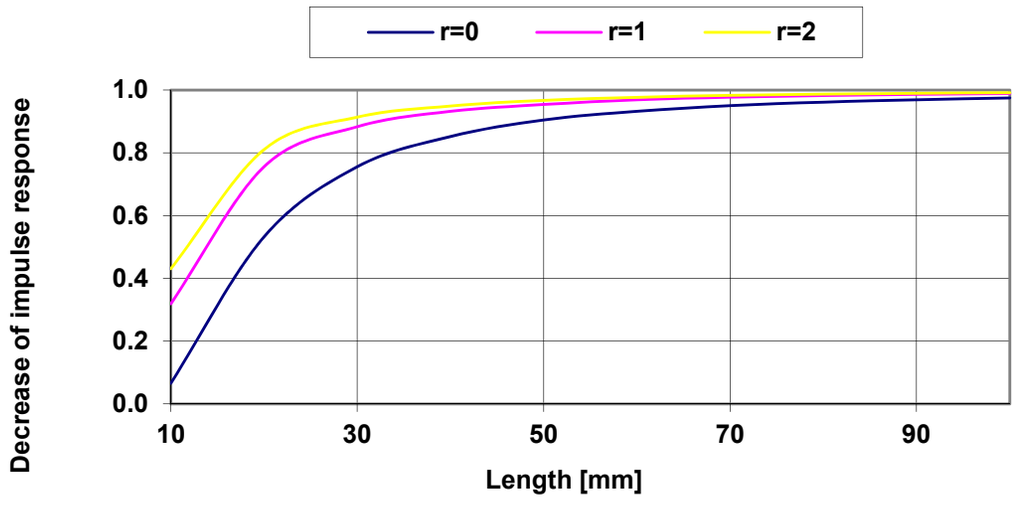

Figure 11. Relative decrease of impulse response amplitude after the time equal to its period in form of a function of plate length for different concentrated mass quantities (r).

damping of free vibrations of the plate is relatively slow. The impulse response of shorter plates is dampened relatively fast. This is why it seems to be beneficial to use possibly long plates loaded by concentrated mass equal to plate mass. The value of resonance frequencies of plates possible to manufacture has changed. It seems that the range of resonance frequency plates available to use is limited to the scope from 20 Hz to 250 Hz. The parameters of resonance frequencies of the plates in the aforementioned range are shown in Figure 12.

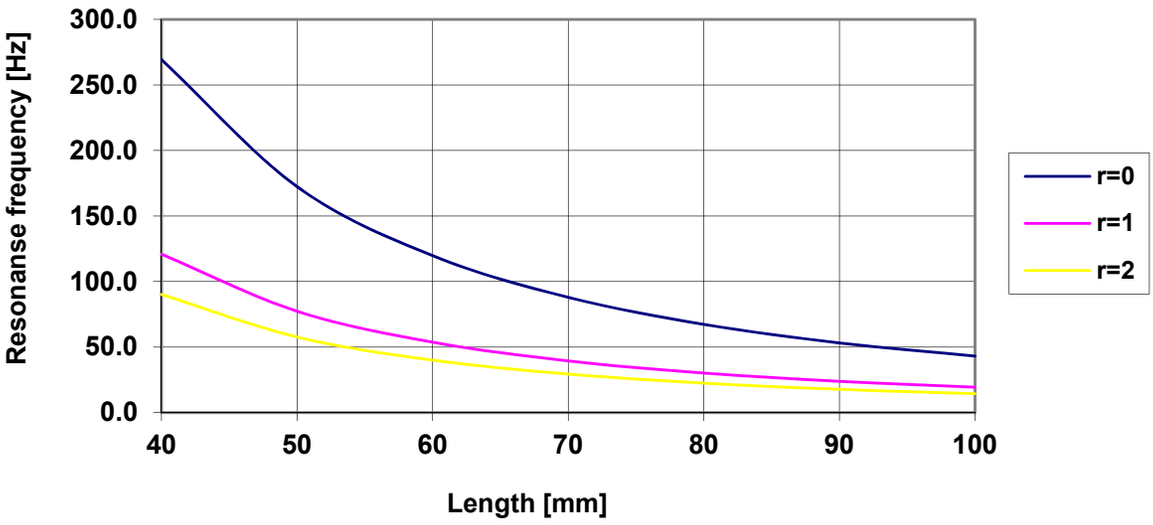

Figure 12. The relation between resonance frequency of a sensor plate and plate length and the value of concentrated mass.

From the above considerations one can draw a conclusion that working with SAW vibration sensors one can utilise their pulse responses or forced vibrations. The sensor resonance characteristics is a basic parameter of the first operation mode. On 0.5 mm thick quartz plates with a concentrated mass equalling the mass of a plate we can achieve plate own vibration frequencies from 20 Hz thru 250Hz. In the second operation mode the vibration sensors with SAW will operate like classical acceleration sensors. The plate resonance frequency should be above the measuring range of a sensor.

The knowledge of the resonance characteristic curve is required for both sensor operation modes. That characteristic can be easily calculated with the aid of the presented model. In the Section 4 we will present experimental examples of the operation of a seismic vibration sensor with SAW, which will enable to evaluate the precision of this model and its usefulness.

3. Vibration sensor electronic components

In order to ensure the transmission of test and supply signals through one coaxial cable there must be a system at the sensor input separating the test signal (74MHz) and supply signal 12VDC (separator). At the output there must be a system summing up the test signal

with a constant supply voltage (adder). Test signal (high frequency) after going through SAW delay line must be amplified to input quantity. It will ensure loss compensation caused by SAW delay line. In the entire line of high frequency test signal (74MHz) a characteristic impedance of 50Ω should be retained. Input and output impedance must have the value of 50Ω. Figure 13 shows the basic functional elements of SAW vibration sensor. Depending on the function in the whole system the following components may be distinguished:

- system separating and summing up the test and supply signals;
- systems adjusting the impedance of SAW line to 50Ω;
- SAW delay line;
- amplifier compensating losses caused by SAW delay line.

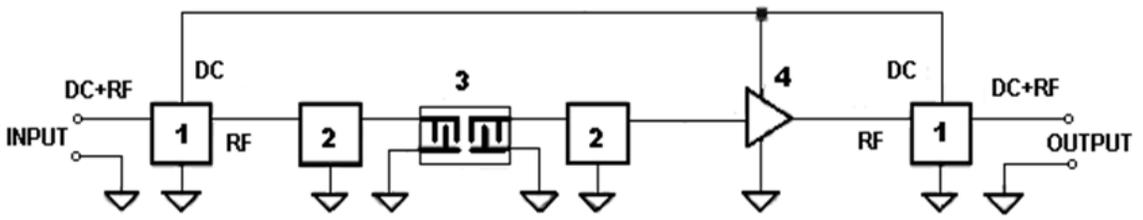

Figure 13. Block diagram of SAW vibration sensor.

The method of making the aforementioned components will be discussed in the next Section.

3.1. System separating or summing up electrical signals (separator/adder)

A system separating test and supply signals is placed at the sensor input. A system summing up these signals is placed at the sensor output. Figure 14 shows a system separating or summing up test and supply signals. The system is in a form of a circulator. It is connected to the line of high frequency signal with a characteristic impedance of 50Ω. A point of separation (or summation) of signals is the place where additional impedance is added to a line of characteristic impedance of 50Ω by inductance L_1. It may change the characteristic impedance of the line and be the reason of signal reflections. In order to avoid this the quantity of added impedance must be much larger than line characteristic impedance (50Ω). In order to fulfill this requirement inductance L_1=4,7uH of its own parallel resonance frequency of 74MHz has been chosen. Figure 15 shows inductance equivalent system diagram.

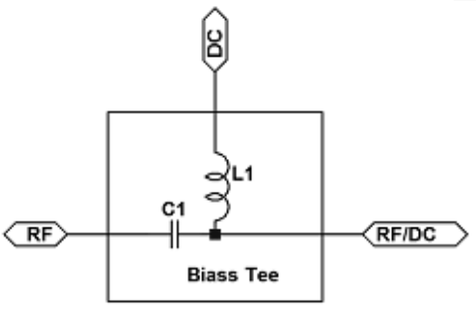

Figure 14. System separating or summing up test and supply signals.

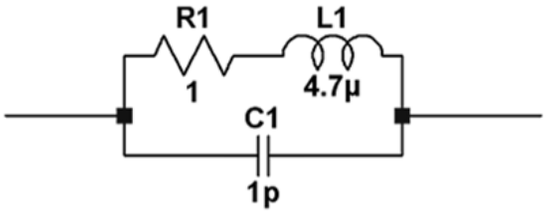

Figure 15. Inductance equivalent system diagram

In reality, the chosen inductance is a parallel resonant circuit. Figure 16 presents change in impedance of such a system in frequency function.

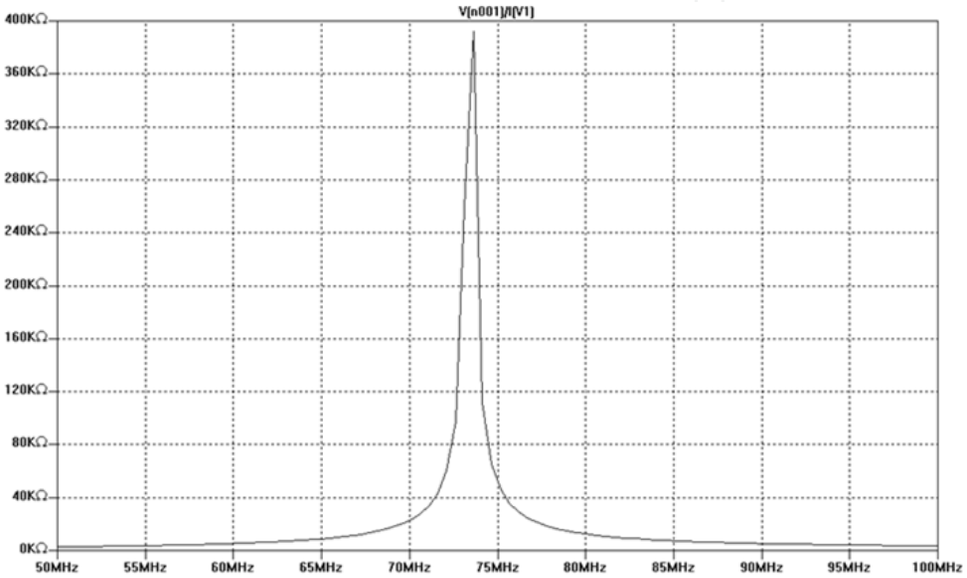

Figure 16. Relationship between impedance and frequency of a system presented in Figure 15

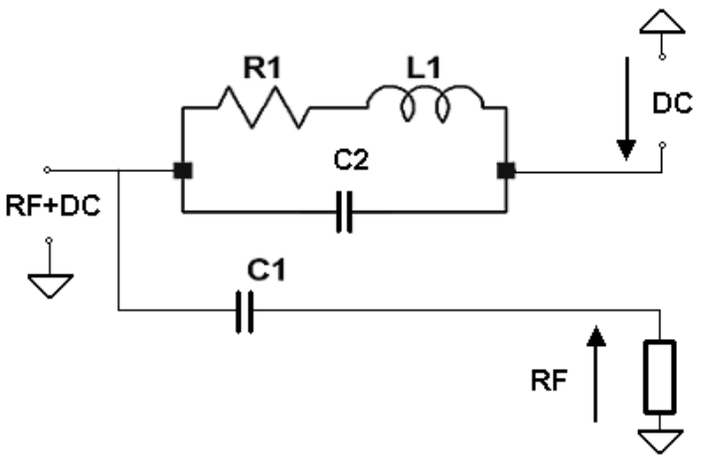

Figure 17. Actual system separating the test and supply signal.

For frequency equal to 74MHz the system impedance value amounts to 400kΩ. It is relatively high in comparison with characteristic impedance of the test signal transmission line (50Ω). It is then possible to obtain considerable attenuation of the test signal entering the supply circuit and it practically eliminates reflections at the point of signal separation or

summation. Figure 17 presents an actual system separating the test and supply signals. Impedance of connected in series: C1 capacity and RF output impedance is equal to characteristic impedance of 50Ω. A diagram presented in Figure 17 enables to analyze test signal attenuation in supply circuit. It allows to calculate the change in line characteristic impedance made by the separating system.

Figure 18 shows attenuation of the test signal at DC output and change in line impedance in frequency function for R1=1Ω.

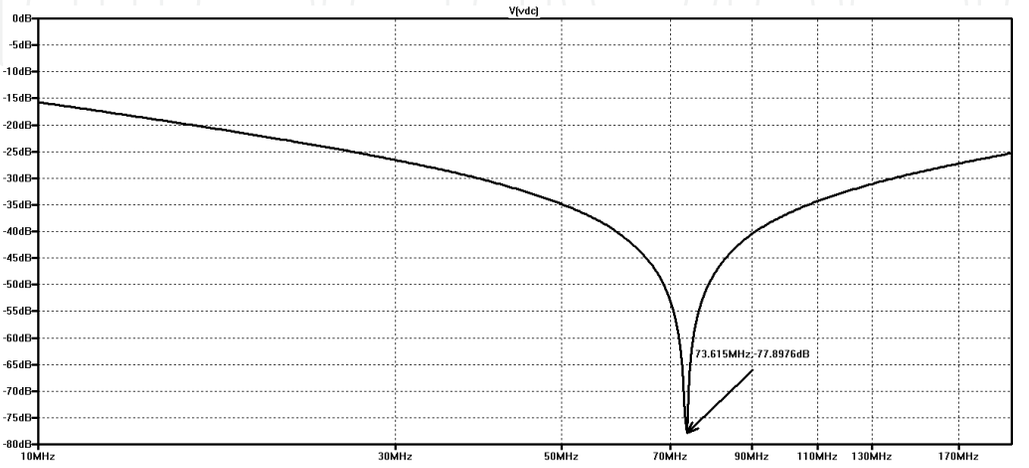

Figure 18. Attenuation of test signal at DC output vs. frequency

Calculations of transmission line impedance change have been done on the assumption that the test signal line has the impedance equaling 50Ω in the entire frequency range. This assumption is correct in the range of line frequency. It substantially simplifies modelling of the system. Figure 19 shows the change line characteristic impedance vs. frequency for R1 = 1Ω.

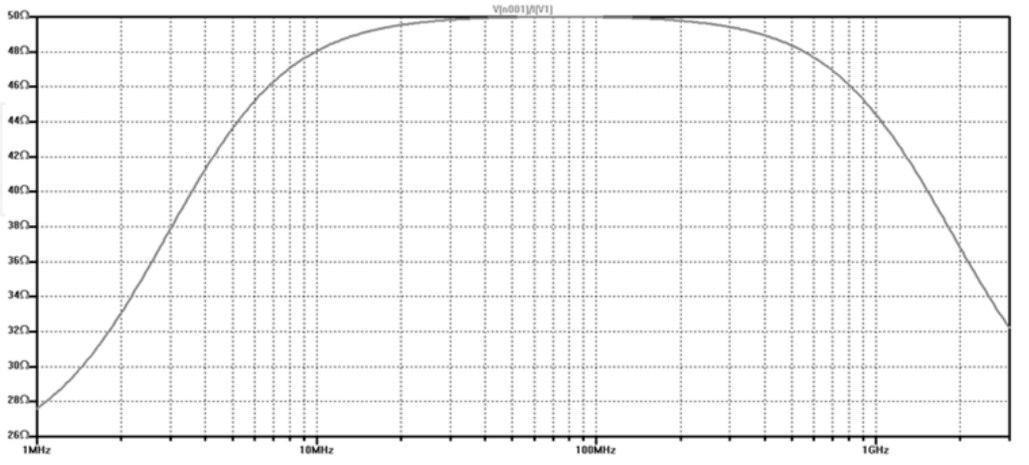

Figure 19. Change in test signal line characteristic impedance in frequency function.

This simplification does not influence the results in the system frequency range. For the sensor frequency equalling 74MHz the test signal attenuation at DC output equals –78dB,

and line impedance equals 50Ω. A separating or summing up system prepared in such a manner does not influence the test signal transmission through SAW vibration sensor.

3.2. Delaying line and adapting system

The design of SAW-comprising delaying lines used for vibration sensors (Figure 20A) differ from those used for sensors of other physical quantities (Figure 20B). Since the sensor plate moves, electrodes applying electric signals to converters (bus bar) should be situated on the immobile part of the plate. (Thus a proper strength of electric contacts for these electrodes will be ensured.) Electrodes are long and their resistance is specific. As the plate moves its housing is greater than that of classic filters comprising the SAW. This causes the signal passing directly between the SAW-comprising delaying line inlet and outlet to increase.

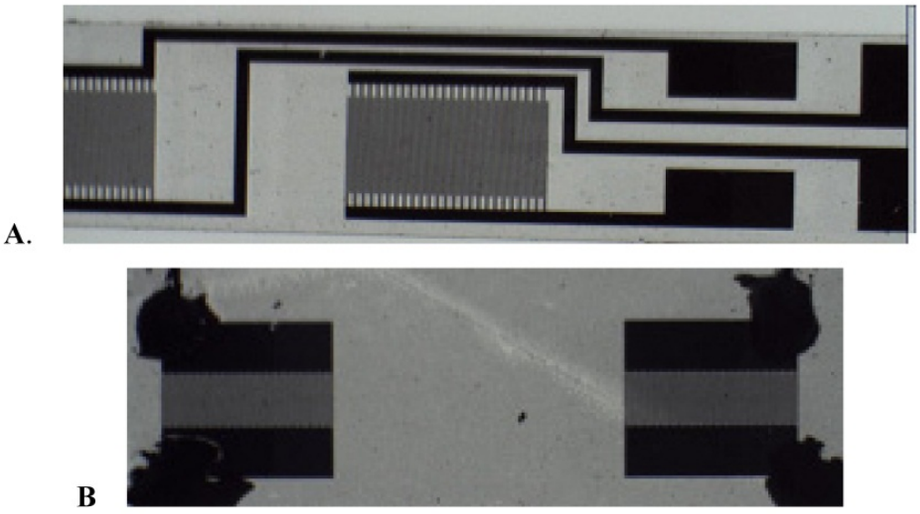

Figure 20. SAW delay lines: for vibration sensor (A), classic (B)

The line was designed in the form of two cooperating, identical, simple, periodical, double-electrode interdigital transducers. Figure 21 shows a system of converter electrodes. Such a structure of converters enables their operation on the third harmonic. The lines were designed to fabricate them with a ST-cut quartz.

Figure 21. Structure of delaying line converters

Due to a low value of the electro-mechanical coupling factor for a ST-cut quartz losses for a mismatch its inlet impedances to 50Ω are significant. In order to cut on these losses

operation of interdigital transducers under conditions of matching to impedance of 50Ω at a frequency of 74MHz was selected [29-32]. Figure 22 shows a converter matching system. The element for matching a converter having the conductance of G_p and the capacity C_p to the impedance $R_g = 50\Omega$ is the inductance L_1. The matching takes place on the condition that the available power derived from a voltage source E_g of the internal impedance $R_g = 50\Omega$ is distributed released/emitted on the converter conductance G_p.

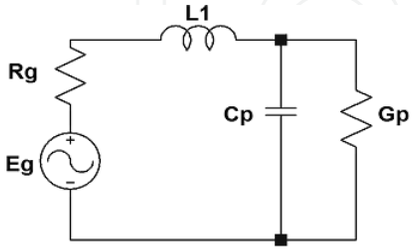

Figure 22. Interdigital transducer matching system to 50Ω impedance..

This condition is met for a conductance resulting from the relationship [29]:

$$L_1 = \frac{C_P}{G_P{}^2 + \omega^2 C_P{}^2} \tag{26}$$

With the help of the (26) relationship the converter geometry for a ST-cut quartz was determined. The aperture of the converter A= 2,5 mm was adopted. To fulfill the purpose converters operated on the third harmonic at 74MHz. For such parameters a converter consisting of N=25 pairs of electrodes was received. The electrode width and the gap between electrodes were 16 μm, and the surface length 37 μm. The results of theoretical calculations of conductance and converter capacity versus frequency are presented in Figure 23.

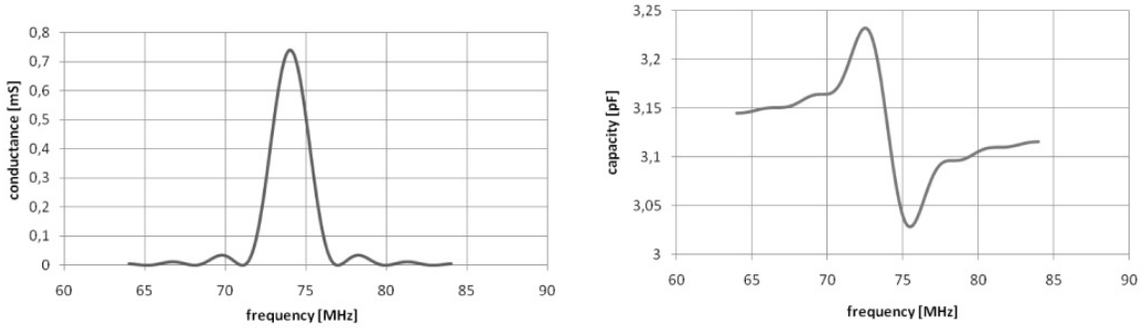

Figure 23. Theoretical dependence of conductance and capacity of simple transducer composed of 25 double electrode pairs on ST-cut quartz.

At 74MHz frequency the converter conductance is 0.74mS and the capacity 3.13pF. For these quantities the inductance L_1= 900nH was calculated, at which value the condition of matching the converter to the impedance 50 Ω is satisfied. Practically, the matching of interdigital transducers to the impedance of 50 Ω was carried out by measurement of the coefficient of reflection Figure 24 shows the change in the coefficient of reflection from a matched converter versus frequency in a system of an impedance of 50 Ω.

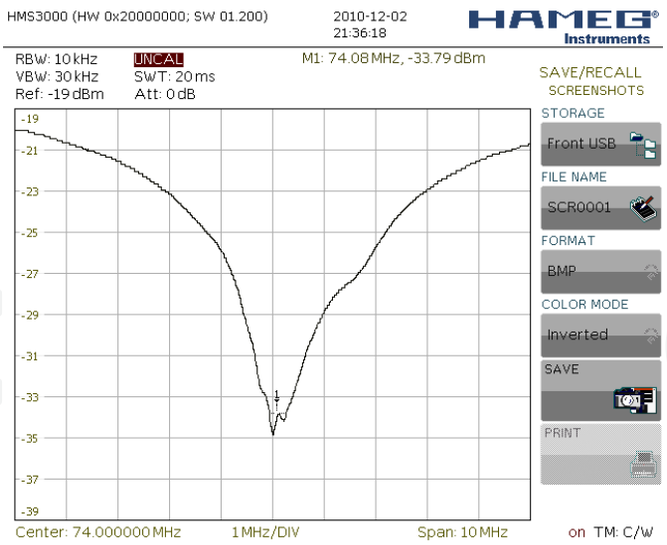

Figure 24. Coefficient of reflection from a matched converter versus frequency.

Figure 25 shows the mounting of the sensor plate.

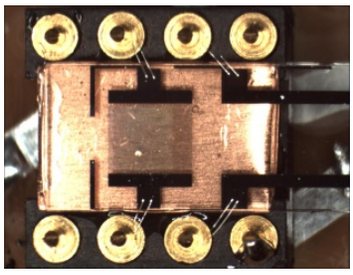

Figure 25. Mounting of the sensor plate

Figure 26 presents the frequency amplitude curve for the fabricated SAW delaying line. The measurement was conducted after the line was mounted in an SAW-based vibration converter.

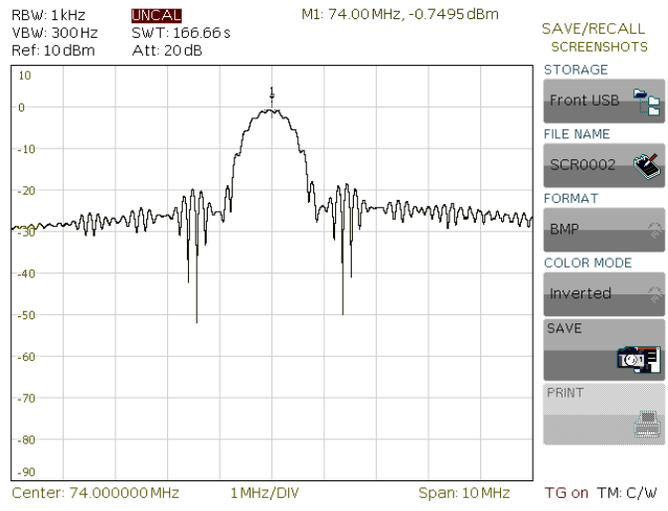

Figure 26. Attenuation frequency diagram of SAW vibration sensor.

3.3. Amplifier

The role of an amplifier is to compensate losses caused by SAW delay line. An amplifier has been built on a monolithic system MAR-6 manufactured by Mini-Circuits. Figure 27 shows a diagram of an amplifier being a part of an electronic system of SAW vibration sensor.

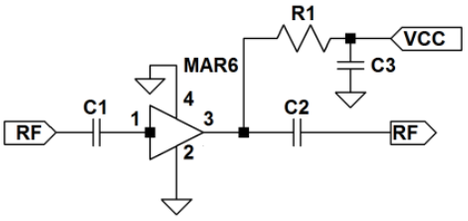

Figure 27. A diagram of an amplifier for SAW vibration sensor.

The amplifier is supplied at the output side by an R1 resistor. The R1 value is selected according to the DC supply voltage. For a supply voltage of 12V the resistance R1 equaled 560Ω. An amplification of 22dB was achieved for test signal frequency of 74MHz. It is the highest amplification value possible to achieve in this system. The value of current input equaled 16mA. Figure 26 shows an experimental frequency characteristics of SAW vibration sensor. Measurement of attenuation frequency diagram of SAW vibration sensor has been conducted on a spectrum analyzer HMS 1010. A supply voltage system has been put at line input. A supply voltage blocking system has been put before the analyzer at line output. Losses of 0.75dB consist of line losses and losses in the connection wiring and discussed separation systems. The value of these losses has been estimated at the level of 1dB. A conclusion may be drawn that an amplifier compensates the losses caused by SAW delay line. A theoretical shape of attenuation frequency diagram of a sensor should be described by the function (sin(x)/x). An experimental characteristic has high-frequency irregularities. Their reasons are the signals going from sensor output to input, omitting sensor electronic components. This signal amplitude is around –36dB lower than useful signal amplitude. The reason of occurrence of signal going from sensor input to output will be discussed in the next Section.

3.4. Parasitic signals

Parasitic signals are the signals going from electronic system input to output, omitting any component which is a part of the test signal transmission line. It is possible due to the occurrence of a parasitic coupling between any place of electronic system. There are two mechanisms leading to the occurrence of couplings [18][33]. The first one is electromagnetic coupling. The second one is ground current coupling. Figure 28 shows the mechanism of electromagnetic coupling. Red lines indicate paths of electromagnetic coupling which may occur in the electronic system of SAW vibration sensor. Electromagnetic couplings occur in all the electronic components constituting a sensor system. Paths of printed circuit are matched to the impedance of 50Ω. They are simultaneously transmitting and receiving aerials. Their efficiency depends on the path length. A similar role is played by inductances occurring in the system and capacities between paths. In order to reduce the electromagnetic

coupling the inductances should be placed perpendicularly to each other and placed at a distance. These elements define the manner of making of the printed circuit plates. Any problems are solved individually, in accordance with a chosen construction.

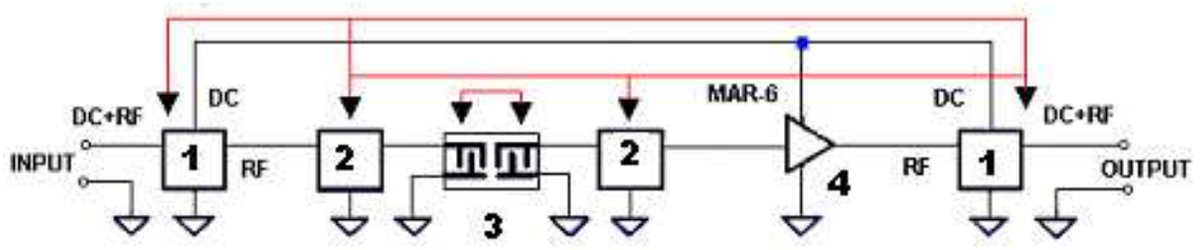

Figure 28. Electromagnetic coupling in electronic system of SAW vibration sensor.

The fundamental problem is an occurrence of electromagnetic coupling between the transducers and SAW delay line. Bus-bars delivering electric signal to transducers are placed on an immobile part of the plate. They are long and they are placed close to each other. It causes an increase in capacity between IDTs. The direct signal going through this way is also strengthened. Because of sensor plate motion its casing is larger than those used in traditional SAW filters. It also causes an increase in direct signal strength in the delay line. This problem and possible solutions are known in literature [29-31]. The most effective solution is symmetrical supply of one of transducers and their functioning in a bridge circuit [34]. Such a solution has been used in the presented SAW vibration sensor. The signal strength at the level of –35dB has been achieved. The second mechanism causing increase in direct signal strength is the ground current coupling [33]. Figure 29 shows the mechanism of this coupling.

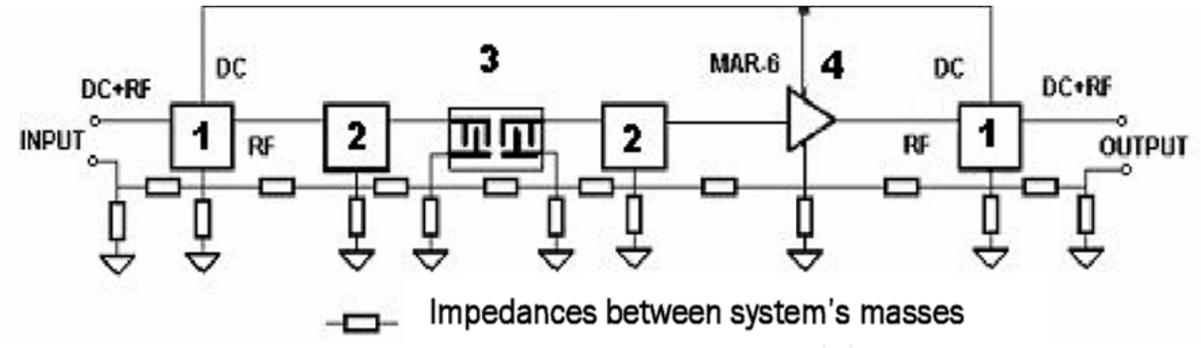

Figure 29. The mechanism of ground current coupling.

Ground current couplings occur only when the connection between component mass and joint mass is not perfect. A diagram in Figure 29 shows this effect by introduced impedances. An ideal connection is characterised by a null value of all impedances. Introduced impedances change current distribution in the entire system. Values of these impedances are small (fractions of ohm). That is why they are difficult to model. A physical making of component mass connection to the system joint mass must be considered during the design stage of the system. Reduction of this value by careful preparation of the system

joint mass is a proper solution. Similarly to the first mechanism, SAW delay line plays an important part. Impedance of bus-bars and impedance of contacts leading the signal to transducer are crucial elements in SAW vibration sensor delay line. The joint mass of the discussed system has been made of 5 mm copper plate to which a printed-circuit board has been soldered. This side of the plate was completely bonded. The electronic system joint mass has been connected to component masses. Figure 30 shows SAW vibration sensor. Only supply voltage of the amplifier system goes through printed circuit paths. Longer segments of test signal line have been made by means of coaxial cables. It allowed to reduce an electromagnetic couplings value in the system. Attenuation frequency diagram of this sensor is presented in Figure 26.

Figure 30. SAW vibration sensor

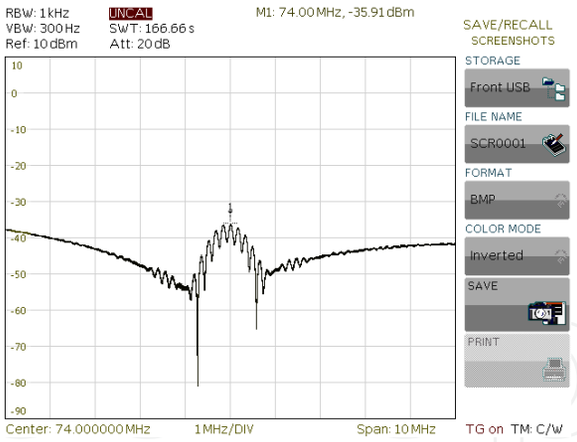

Figure 31. Attenuation frequency diagram of SAW vibration sensor after shut-down of amplifier supply.

Figure 31 presents this characteristic after a shut-down of amplifier supply. Shapes of characteristics in delay line operation band are similar in both figures. It suggests that signal source at the sensor output is situated behind SAW delay line. This signal strength is –35dB below the sensor frequency characteristic signal. Beyond the operation band the signal strength equals –40dB. Conducted measurements make use of the time trace of stationary signals. The lack of information about the delay of these signals does not allow to determine their source. IDTs are selectively matched to the impedance of 50Ω. It can be a signal going

directly between interdigital transducers of SAW delay line. In order to explain the origin of the signal, it is important to learn about its delay time. It has been made in a system presented in Figure 32.

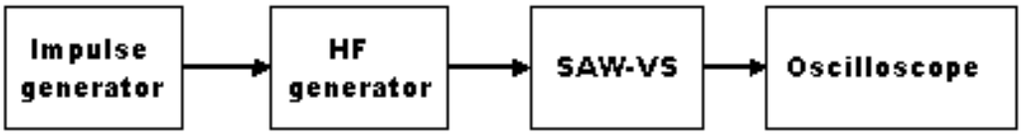

Figure 32. Meter circuit for parasitic signals in SAW delay line.

At sensor input a signal in form of wave packet at frequency of 74MHz has been delivered. The length of the packet is smaller than line delay. In this way a temporary separation of the direct and useful signals has been ensured.

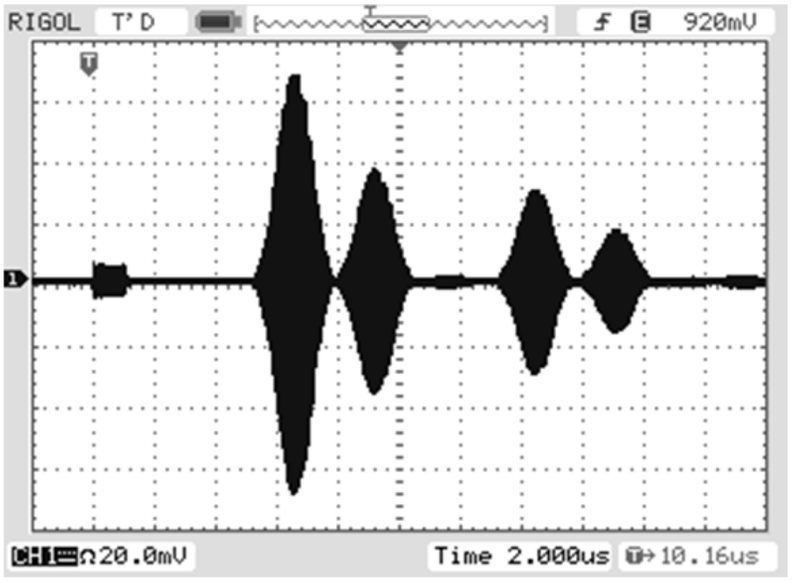

Figure 33. Time run of signals in SAW delay line.

Figure 33 presents timing of signals at the output of SAW vibration sensor. There are five signals at the sensor output. The first signal is going directly from sensor output to its input. The second one is a useful signal. Next three signals are reflected from the plate edge. Reflected signals will be attenuated by a damping paste. The amplitude of direct signal is – 35dB below the useful signal. It leads to conclusion that the signal shown in Figure 31 is a signal going directly between SAW delay line IDTs. When the electronic system is properly made, the elimination of this signal is the most fundamental problem in SAW vibration sensor design.

4. Measurements of vibration sensor parameters

SAW-based vibration sensors with SAW were made as described in Section 3. Delaying lines of a 74MHz middle frequency and various delay quantities of 4.2μs, 6.2μs, 8.2μs were

worked out. These delaying lines were made on ST-cut quartz plates of different lengths. These plates were 5.7 mm wide and 0.5 mm thick.

The signal passing thru a sensor is continuous one. In a sensor every parasite signal adds up to a useful signal and causes the amplitude of a useful signal to modulate. This causes the sensor sensitivity to decrease; therefore parasitic signals must be removed. An essential problem is the reduction of a signal passing directly from the delay line inlet to the delay line outlet. The magnitude of this signal for sensors with lines of different delays is shown in Figure 34. The larger the line delay the lower the direct signal level. This level depends on the outlay of electric inlets to the delaying line converters. This is illustrated in Figures 35 (oscilloscope signals A and C). In order to lower the direct signal level additional screening of interdigital transducers or a symmetric supply of one of the converters was used [34]. For executed sensors a direct signal at a level of –36dB was obtained.

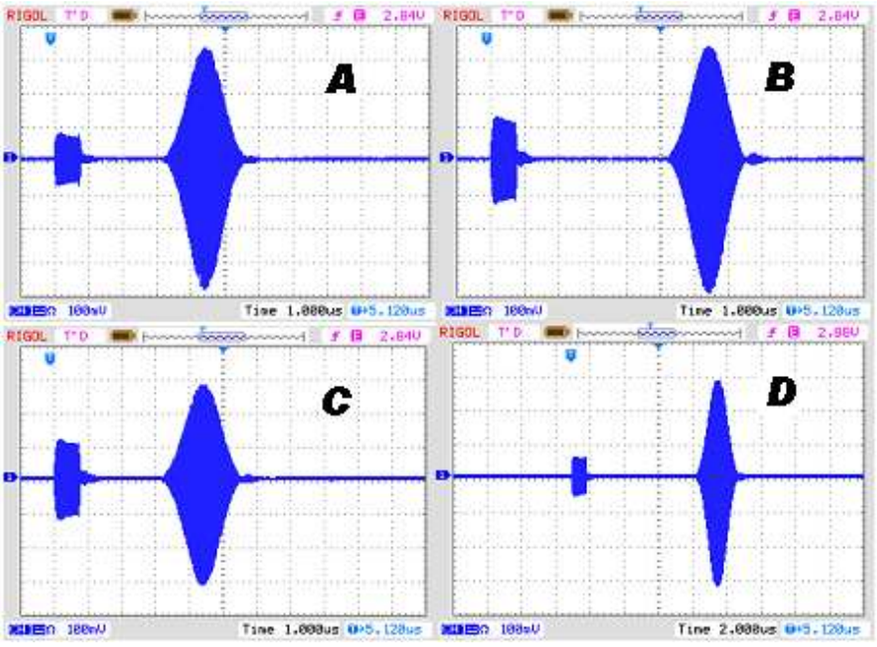

Figure 34. Direct and useful signal in delaying lines of different delays: A – 4,2μs, B – 6,2μs, C – 4,2μs, D – 8,2μs.

To basic parameters of vibration sensors belong their frequency characteristic curves and the static sensitivity. We will present the way they are measured. Determined experimental characteristics will be compared to the theoretical one. This will enable to estimate the model precision and to what extent it can help to model the parameters of SAW-based vibration sensors. The sensor frequency characteristics were determined in two stages. At the first stage the sensor pulse response was registered. At the second stage the spectrum of this pulse response was determined. Its shape corresponds with the sensor frequency characteristics. Pulse responses of sensors were measured and recorded as well as the spectrum of pulse responses from sensors were calculated with the aid of the system shown in Figure 35. Sensors were agitated for vibrations by an impact. Pulse responses were recorded with the help of the Agilent VEE Pro programme.

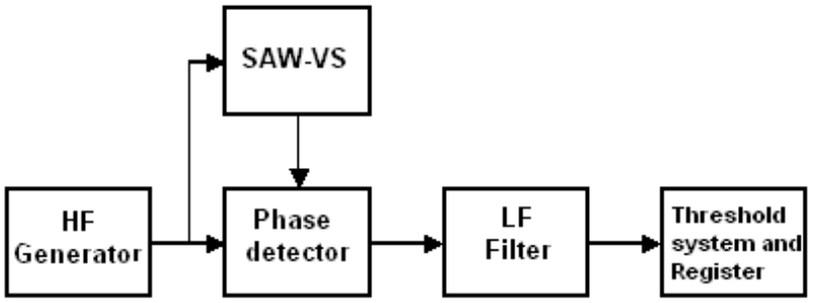

Figure 35. System to measure responses from SAW-based vibration sensor pulse plates.

Figure 36 presents a pulse response of a sensor where a delaying line with a 65 mm long plate was used. The sensor plate was not loaded with a seismic mass. The length of the pulse response was approximately 5s and its frequency was 92Hz.

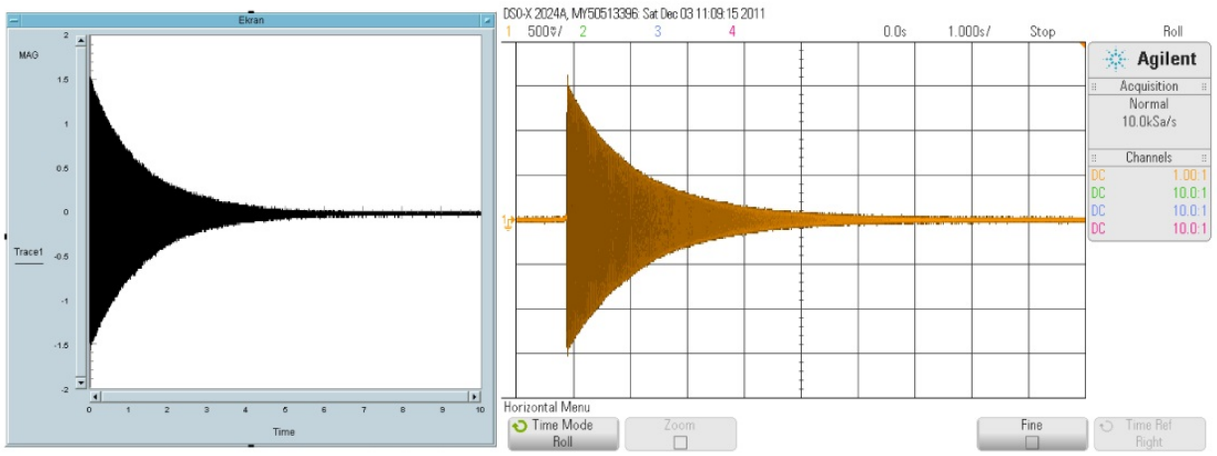

a. b.

Figure 36. Pulse response of sensor with 65 mm long plate without seismic mass recorded with VEE programme – (a) and oscilloscope – (b)

The spectrum of a pulse response (a Fourier transform) was calculated with the help the Agilent VEE Pro programme, but it can be achieved also directly on an oscilloscope. Figure 37 presents the amplitude of this spectrum. Its shape corresponds to the amplitude of the frequency characteristics of a tested sensor. The resonance frequency equals theoretical values calculated with the relationships presented in Section 2. The frequency characteristics shows a harmonic at a 400Hz frequency. Its level is –26dB below the level of the sensor characteristics for the resonance frequency. This level is higher than its theoretical estimate presented in Section 2. It is difficult to determine the reason for this difference. It can be the inaccuracy of the model. However, it can be also due to a differing effectiveness of incitation of the resonance frequency component and harmonic frequency component.

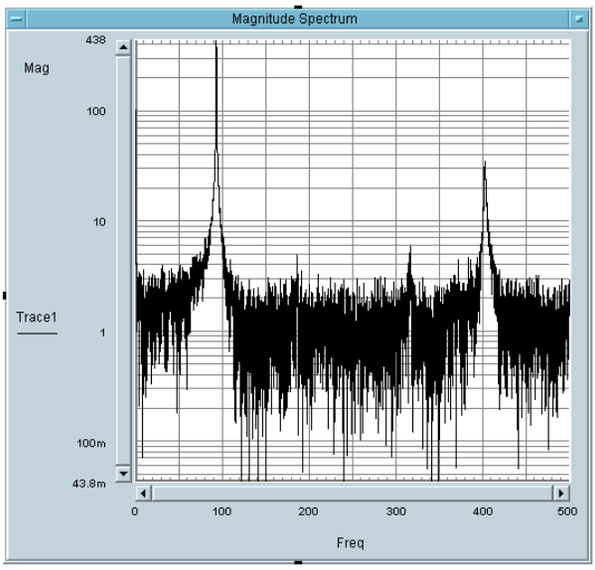

Figure 37. Spectrum of sensor with 65 mm long plate without seismic mass

Figure 38 presents the measurement of the statistical sensitivity of a sensor. It was conducted by recording the sensor output signal during its rotation by 180 degrees. This rotation causes the constant acceleration affecting a sensor to change by a value of two gravitational accelerations – i.e. 2 „g". An estimated static sensitivity of a sensor is 40mV/(„g").

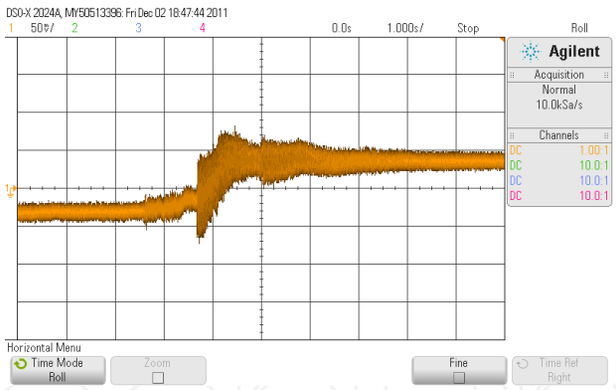

Figure 38. Method of determining static sensitivity of sensor

A 1.07g (r=2,27) seismic mass was placed on a sensor. This caused its resonance frequency to drop to 29Hz, and then for this sensor the above-presented tests were repeated. Fig. 39 shows the pulse response of a sensor with a 65mm long plate with a 1.07 g seismic mass. The pulse response is longer than 10s, with its frequency being 29Hz.

Figure 40 shows the frequency characteristics of the tested sensor. The value of the resonance characteristics equals the theoretical value. The characteristics shows a harmonic at 58Hz. Its level is –4dB below the sensor characteristic value for the resonance frequency, and being low, practically has no impact on the sensor function. Figure 41 shows the measurement result of the sensor static sensitivity as 100mV/(„g"). Against a sensor without a concentrated mass this value rose 2 ½ times. The length of the pulse response increased

more than 2 times. These changes are obvious and their quantities determine explicit relationships describing the sensor model. The only difference between the results of experimental tests against the theoretical model is a higher level of the harmonic resonance frequency. To explain this difference classical measurements of the sensor resonance characteristics must be conducted. To conduct these measurements an exciter of stable mechanical vibrations of the sensor housing of an adjusted amplitude and frequency is required. It was not possible for the authors to carry out these tests.

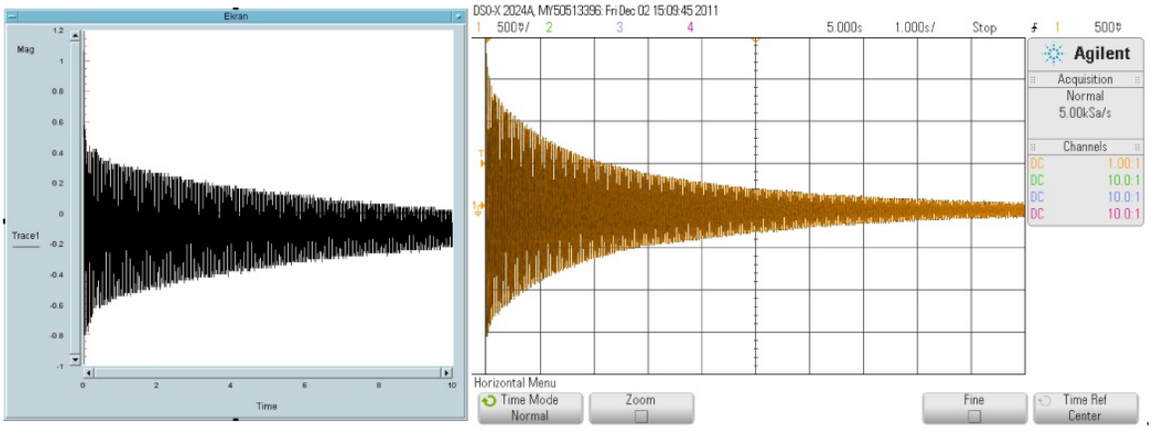

a. b.

Figure 39. Pulse response of sensor with 65 mm long plate with a 1.07g seismic mass recorded with VEE programme – (a) and oscilloscope – (b)

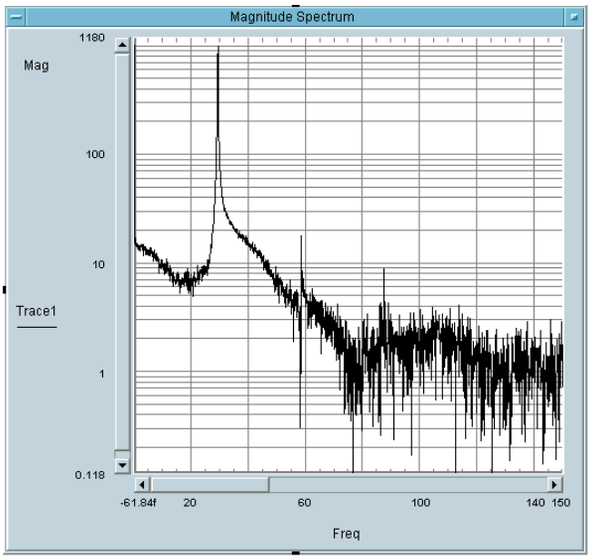

Figure 40. Spectrum of a 65mm long sensor with 1.07 g seismic mass

The test results demonstrated a good compatibility between the theoretical parameters of the sensor pulse response (resonance frequency and the decay time) and their experimental realization. The model presented in Section 2 was used to elaborate SAW-based sensors, which featured required parameters of the pulse response. Figure 42 shows a block diagram of an electronic warning system with SAW-based vibration sensors.

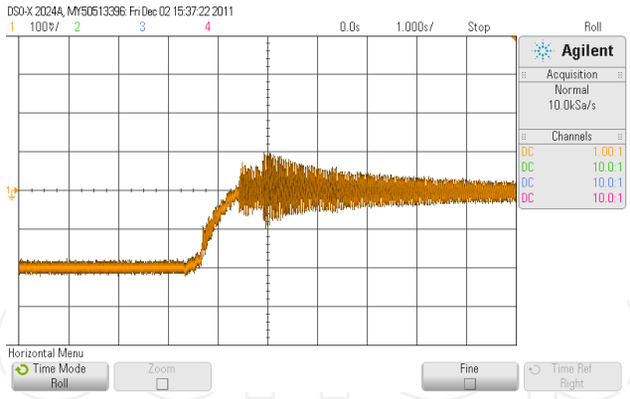

Figure 41. Method of determination the sensor static sensitivity

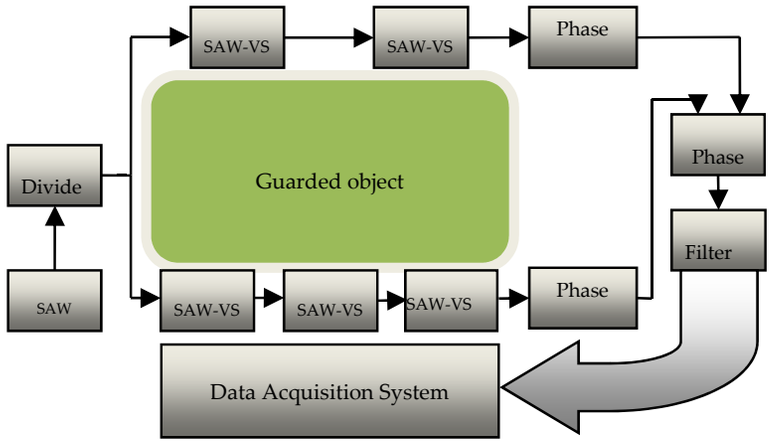

Figure 42. Block diagram of electronic warning system with SAW-comprising vibration sensors.

During operation of the system vibratons of the sensor plate change the phase of the measuring signal. The frequency of these changes equals the plate resonance frequency. Thus the signal from every sensor passing thru a set of filters at the phase detector inlet can be separated. The system operation is discussed further in the following works [35][36]. The said system required SAW-based vibration sensors having parameters given in the Table 2; the authors prepared these sensors.

Sensor No.	1	2	3	4	5
Resonance frequency [Hz]	41	56	73	90	159
Plate length [mm]	86	85	66	68	26
Seismic mass - r	0.22	0	0.14	0	1
Line delay [μs]	6.2	4.2	8.2	4.2	4.2

Table 2. Parameters of SAW-VS sensors made for electronic warning system

By selection of a seismic mass required resonance frequencies of sensors were achieved. In case of sensors No. 1 and 2 as well as No. 3 and 4 plates of similar lengths were used. Figure 43 presents characteristics of four assembled sensors.

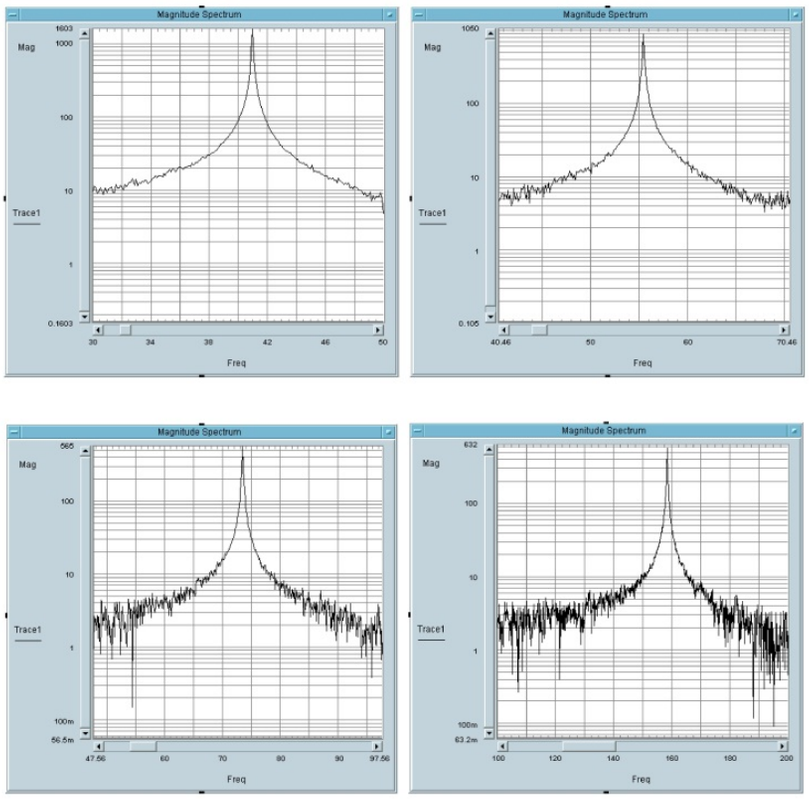

Figure 43. Frequency characteristics of sensors of resonance frequency of 41Hz, 56Hz, 73Hz, 159Hz.

These five SAW-based vibration sensors fabricated and used in an electronic warning system proved the efficiency of the presented modeling method. The system was tested on a stand shown in Figure 44. The sensors were attached to steel ropes tensioned as required. In order to describe the movement of sensors and ropes a model of a string loaded with a sensor mass taking into account its moment of inertia [37] was developed.

Figure 44. SAW-comprising vibration sensors attached to steel ropes

Vibrations of sensors were stimulated by deflecting them out of the state of equilibrium. The string vibration time was several times as long as that of the decay time of a senor plate

pulse response. The movement of a sensor was a sum of the fading with time of the pulse response and vibrations enforced by a cyclic movement of the sensors housing. The frequency of the housing movements was that of the rope vibration frequency, which was selected so that it was lower than the resonance frequency of sensors. Thus it was possible to analyze every component of the sensor movement. For experimental testing a string vibration frequency of some 6 Hz was chosen. For every sensor the output signal from the phase detector (Fig. 42) was recorded and processed with the VEE program. Figure 45 and 46 show the course of signals of vibrating sensor of various resonance frequencies and their spectra.

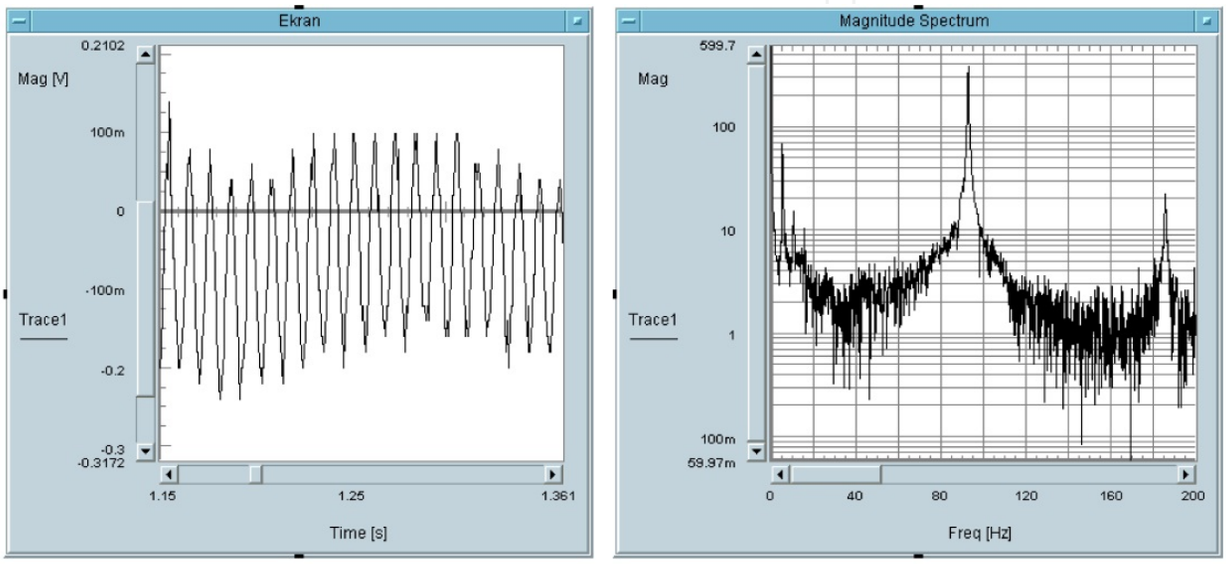

Figure 45. Part of output signal from sensor of plate resonance frequency of 91 Hz and string vibration frequency of 6.7 Hz and its spectrum

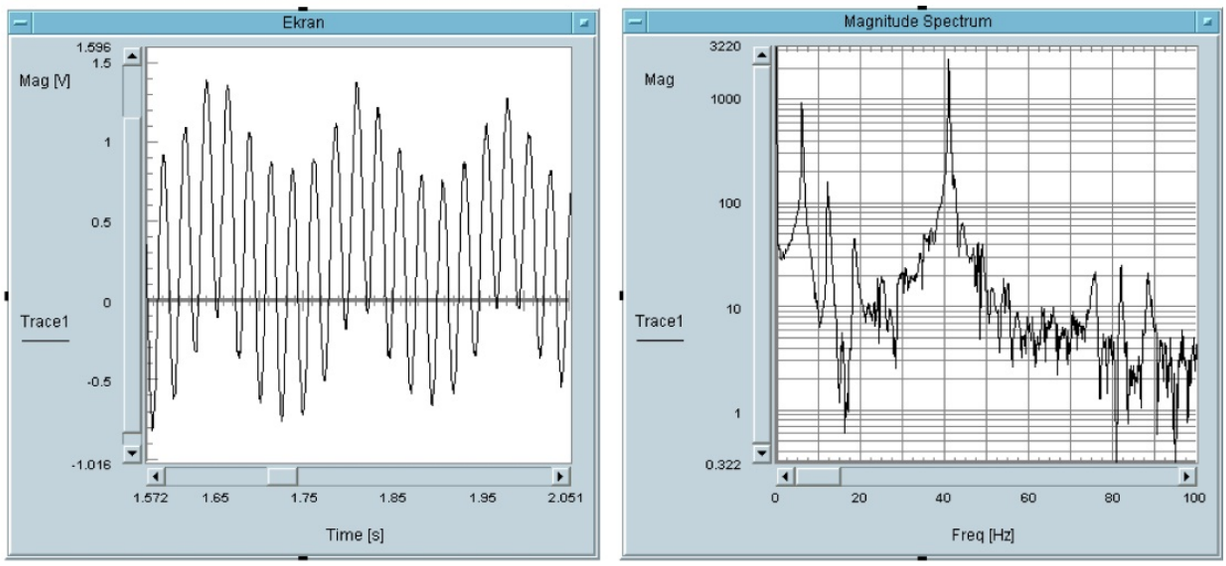

Figure 46. Part of output signal from sensor of plate resonance frequency of 41 Hz and string vibration frequency of 6.7 Hz and its spectrum

Pulse responses of sensors of an 91Hz (Fig. 45) or a 41Hz (Fig. 46) frequency can be easily discerned form signals derived from a string movement of a 6.7 Hz frequency, especially within the signal spectrum. Relations between their amplitudes are visible. After decay of pulse responses sensors measure the rope vibrations; they work then like classical vibration sensors.

In case of a sensor plate without the seismic mass (Fig. 45) the harmonic amplitude occurs at the – 34dB level below the resonance frequency amplitude. With the plate loaded with a small seismic mass (r=0,22, Fig. 46) the level is lower than -40dB. Harmonic vibrations had no impact on the operation of a system presented in Figure 43.

Depending on the use of a sensor by selection of its resonance frequency we can change its sensitivity and linearity. The practically prepared electronic warning system with SAW-based vibration sensors has fully proven the usefulness of the model presented in Section 2.

5. Conclusions

The work presents development, execution and parameters of SAW seismic vibration sensors. A sensor is a two-terminal pair network consisting of a delaying line with SAW and an amplifier compensating losses introduced by a ST-cut quartz. The delay line is fabricated on the CT-cut quartz surface.

A simple vibration model of an anisotropic plate was used to develop sensors. By way of successive simplifications of the description of vibrations of a viscous-elastic sensor plate a model of one degree of freedom was obtained. An explicit description of the movement parameters of the sensor plate was achieved. A material damping of the plate practically causes it to vibrate at only one resonance frequency, thus enabling to design SAW seismic vibration sensors. The results of experiments proved the effectiveness of using this model to design SAW-comprising seismic vibration sensors.

Basic parameters of realised vibration sensors (resonance characteristics, pulse responses, static sensitivity) are presented and analysed.

The range of resonance frequencies of plates made of ST-cut quartz, which were feasible, was determined. The plate length restricts the lower range of resonance frequencies. This range was determined on the basis of an available length of 100mm of a CT-cut quartz. The upper range of resonance frequencies is restricted by the speed of decay of a pulse response of a sensor plate. However, this restriction applies only to a sensor operating on its pulse responses. For the determination of this range the magnitude of stresses occurring in the plate was not taken into account. This magnitude must be smaller than the size of critical stresses presented in Table 1. In the subject work this element was not analysed. The magnitude of dynamic, critical stresses for a ST-cut quartz was determined in works [22] [23]. These values do not conform to standards and they apply to a series of plates cut out with a wire saw. In the course of that determination it turned out that the technology of plates production has a great impact on the value of dynamic critical stresses. The work [18] demonstrated that their value for a given design of a sensor does not restrict the determined range of the plate resonance frequencies.

As the plate resonance decreases the sensor sensitivity increases. Therefore high sensitivity sensors can be designed. Increasing its length can lower the resonance frequency of a plate. This is the most effective way to reduce the plate resonance frequency. It is possible to develop high-sensitivity vibration sensors of resonance frequencies in the order of a few Hz. To design such sensors one can use directly the presented model. Lets compare the SAW (SAW-VS) vibration sensor presented in the work to three kinds of sensors used at present. Resonance frequencies and basic applications of these sensors are presented in the introduction to this work.

The first kind of these sensors is geophones, where the sensor pulse response is utilized, which explains their low resonance frequency (several Hz) and a high sensitivity.

The two remaining kinds of vibration sensors are micro-mechanical silicone acceleration sensors (Micro Electro Mechanical Systems accelerometers - MEMS accelerometers) and piezoelectric acceleration sensors. Lets compare the basic parameters of these sensors: sensitivity, range of measured values and the frequency of acceleration changes, their structure (resonance frequency (natural frequency), weight and the manner of measuring the acceleration. We don't compare acceleration sensors reacting to impacts. They are very light and feature a very broad measuring range. Piezoelectric acceleration sensors work within a range between fractions of Hz thru a dozen or so kHz. The lower and upper range of the measurement dynamics is from 1 "mg" up to 100.000 „g". („g" is a unit of acceleration equal to the gravitational acceleration at sea level, i.e. 9.81m/s^{-2}). Depending on the design the sensor sensitivity is 0.2mV/g - 0.7V/g. The natural (resonance) frequency ranges from a few Hz to a few dozen of Hz. These sensors weigh from 3g to 500 g. The structure of these sensors is relatively simple, however, the measuring system is complicated (measuring of charge changes in the order of pC). MEMS accelerometers are characterized by small dimensions (an integrated circuit) and a low price. With these devices constant and variable acceleration up to a frequency of a few hundred Hz can be measured.

The lower and upper range of the measurement dynamics is from fractional „g" to 10 000 „g". Depending on the design the device sensitivity ranges from 0.2mV/g up to 10V/g (this applies to seismology sensors).

The device resonance frequency (natural frequency) is high: several Hz. These devices weigh from a few g up to 2 500 „g" (in case of seismology sensors). The sensor design is relatively simple; as well its measuring system is simple. (Measuring of changes in the charge in the order of aF's.)

The measuring system of a MEMS sensor is similar to a measuring system of an SAW-vibration sensor presented in the work (Figure 35). It consists of a measuring generator of a 1MHz frequency, two measuring paths and a phase detector.

The mechanical frequency of SAW-comprising vibration sensors can be changed within a range from several to a few hundred Hz. This is a significant difference between these both kinds of sensors. The sensitivity of an SAW vibration sensor depends on the resonance characteristics of the sensor plate, the length of the surface wave utilized in a sensor and on the sensor design. One can define here the sensitivity for a constant acceleration and the

sensitivity for the resonance frequency of the sensor plate or some other frequency. For comparison's sake we can assume the sensitivity for a constant acceleration.

An example: for a SAW-VS with a plate 57.5 mm long and 0.5 mm thick, loaded with a seismic mass equal to 4 times the plate mass, a static sensitivity of 0.5V/„g" was achieved. The sensitivity of SAW-sensors for changing accelerations can be a couple of times greater than that for constant accelerations. The sensitivity degree is determined by the resonance curve of a sensor plate. The sensitivity of vibration sensors with SAW-VS can be increased by decreasing the length of the surface wave, or changing the sensor design (i.e. reduction of the plate thickness), by increasing the concentrated mass or by increasing the delay of the SAW-delaying line.

SAW vibration sensors can be cascaded which offers many system designs what in turn offers an increase in the sensitivity and a reduction of the cross sensitivity of sensors. This is not possible with a MEMS sensor and a piezoelectric sensor. The high measuring frequency of SAW-comprising sensors allows designing wireless sensor versions.

In terms of the design and the method of measuring MEMS and SAW-VS acceleration sensors have a lot in common. In a MEMS sensor a vibrating plate of silicon changes the capacity of a capacitor. Mechanical properties of silicon (density 2.330kg/m^{-3}, and an equivalent Young's modulus of 106 Gpa) are similar to mechanical properties of quartz. Therefore the parameters of MEMS and SAW-VS must be similar. In our opinion SAW-VS sensors have their place in the measuring technology.

This work presents an example of using SAW-sensors in an electronic warning system. Vibration sensors placed at selected points record vibrations within areas they cover. An alert central station registers signals from a vibration sensor. This is a typical system to be applied for perimeter protection systems.

All sensors included in a system can be placed within one area; then this system will perform the role of an analyzer of vibrations within this area. This is a second prospective application of the system under discussion. The possibility of preparing high-sensitivity vibration sensors of resonance frequencies in the order of a few Hz is a prospective area of application for monitoring vibrations of bridges and buildings, where the frequency of free vibrations is in the order of fractions of Hz up to a dozen or so Hz. The presented application examples apply to working on the pulse response of an SAW-sensor. This kind of a sensor can be used to measure one component of the acceleration vector. Then, the pulse response means for a measurement of acceleration a parasitic signal, and should be eliminated. Therefore thru the use of sensor plates, where the decay of a pulse response is fast, acceleration sensors can be developed. The movement of a plate shows then a character of acceleration changes in time. Works [38] [39] show development of this kind of sensors.

Author details

Jerzy Filipiak and Grzegorz Steczko
Institute of Electronic and Control Systems, Technical University of Czestochowa, Częstochowa, Poland

Acknowledgement

This work was supported by the Polish Ministry of Science and Higher Education as a project "Vibration Warning System with SAW Vibration Sensors" included in the scientific budget of 2009–2011.

6. References

[1] Pakhamov A, Pisano D, Sicignano A and Golburt T (2005) High Performance Seismic Sensor Requirements for Military and Secuirity Applications Proceedings of SPIE, j. 5796: 117-124.
[2] Kaajakari V, (2009) Practical MEMS, Small Gear Publishing
[3] Lee I.G, Yoon G.H, Park J, Seok S, Chun K, Lee K (2005) Development and analysis of the vertical capacitive accelerometer. Sensors and Actuators A j.119: 8-18.
[4] www.metrozet.com
[5] Wohltjen H, Dessy R (1979) Surface Acoustic Waves Probe for Chemical Analysis I. Introductcion and Instrument Design. Analytical Chemistry. j. 9: 1458-1475.
[6] Nakamoto T, Nakamura K, Moriizumi T (1996) Study of Oscillator- Circuit Behavior for QCM Gas Sensor. Proc. Ultrasonics Symposium.j. 1: 351-354.
[7] Gizeli E, Liley M, Love C.R, Vogel H (1997) Antibody Binding to a Functionalized Supported Lipid Layer, A Direct Acoustic Immunosensor, Analytical Chemistry. j. 69: 4808-4813.
[8] Urbańczyk M, Jakubik W, Kochowski S (1994) Investigation of sensor properties of cooper phtalocyanine with the use of surface acoustic waves. Sensors and Actuators B j.22: 133-137.
[9] Cullen C, Reeder T, (1975) Measurement of SAW Velocity Versus Strain for YX and ST Quartz. Proc. Ultrasonics Symposium: 519-522.
[10] Cullen C, Montress T (1980) Progress in the Development of SAW Resonator Pressure Transducers. Proc. Ultrasonics Symposium. j. 2: 696-701.
[11] Pohl A, Ostermayer G, Reindl L, Seifert F (1997) Monitoring the Tire Pressure of Cars Using Passsive SAW Sensors. Proc. Ultrasonics Symposium.j.1: 471-474.
[12] Clayton L.D, EerNisse E.F (1998) Quartz thicknes-shear mode pressure sensor design for enhanced sensitivity. IEEE Transactions on Ultrasonics, Ferroelectrics, and Frequency Control. J.45: 1196-1203.
[13] Jiang Q, Yang X.M, Zhou H.G, Yang J.S (2005) Analysis of surface acoustic wave pressure sensor. Sensors and Actuators A j.118: 1-5.
[14] Drafts B (2000) Acoustic wave technology sensors. Sensors j.10: 1-9.
[15] Seifert F, Bulst W, Ruppel C (1994) Mechanical sensor based on surface acoustic waves. Sensors and Actuator A. j. 44: 231-239.
[16] Hauden D (1991) Elastic waves for miniaturized piezoelectric sensors: applications to physical quantity measurements and chemical detection. Archives of Acoustics. j. 16: 91-106.

[17] Filipiak J, Solarz L, Steczko G (2007) Surface acoustic wave stress sensors. Desinger Analysis. Molecular and Quantum Acoustics. j. 28: 71-80.
[18] Filipiak J (2006) Surface acoustic wave acceleration sensors. Technical University of Czestochowa. Monograph 121, p.198. (in Polish).
[19] Filipiak J, Kopycki C (1999) Surface acoustic waves for the detection of small vibrations. Sensors and Actuators. j. 76: 318-322.
[20] Filipiak J, Solarz L, Steczko G (2009) Surface acoustic wave vibration sensors for linear electronic warning systems. Acta Physica Polonica A j.116: 302-306.
[21] Filipiak J, Solarz L, Steczko G (2011) Surface Acoustic Wave (SAW) Vibration Sensor. Sensors. j.11: 11809-11832. http://www.mdpi.com/journal/sensors
[22] Filipiak J, Zubko K (2005) Determination of damping in piezoelectric crystals. Molecular and Quantum Acoustics j. 26: 75-80.
[23] Kopycki C (1999) Effect of substrates on the parameters of piezoelectric vibration sensor with a surface acoustic wave. Ph.D. Thesis (in Polish), Military University of Technology, Warsaw,
[24] Nye J.F (1957) Physical Properties of Crystals; Clarendon Press: Oxford, GB.
[25] Mason W.P (1958) Physical Acoustics and the Properties of Solids. Van Nostrand,
[26] Bogusz W, Dżygadło Z, Rogula D, Sobczyk K, Solarz L (1992) Vibrations and Waves A. Elsevier: Amsterdam
[27] Zubko K (2006) Applying of the Rayleigh method to determination of elastic and viscoelastic parameters of piezoelectric crystals. Ph.D. Thesis (in Polish), Military University of Technology, Warsaw,
[28] Filipiak J, Solarz L, Zubko K (2004) Analysis of Acceleration Sensor by the discrete model. Molecular and Quantum Acoustics j. 25: 89-99.
[29] Filipiak J (1993) Problems of synthesis of components of a surface acoustic wave signal processing to complex type "chirp". Ph.D. Thesis (in Polish), Military University of Technology, Warsaw,
[30] Matthews H L (1997) Surface Wave Filters. John Wiley and Sons, New York.
[31] Morgan D P (1985) Surface Wave Devices for Signal Processing. Academic
[32] Ruppel C C W, Fieldly T A (2001) Advances in Surface Acoustic Waves Technology, Systems and Applications (vol 2). Word Scientific Pub. Co. Inc,.
[33] www.saw-devices.com
[34] Danicki E, Filipiak J (1982) Bridging method for elimination of the direct signal, Electronics (in Polish), j.10-12: 22-26
[35] Filipiak J, Solarz L, Steczko G(2011) Electronic Warning System Based on SAW Vibration Sensors, Acta Physica Polonica A j.120: 593-597
[36] Filipiak J, Solarz L, Steczko G(2009) Surface acoustic wave vibration sensors for linear electronic warning systems. Acta Physica Polonica A j.116: 302-306
[37] Filipiak J, Solarz L, Steczko G (2010) Analysis of Experimental Stand for SAW Vibrations Sensor, Acta Physica Polonica A j.118: 1118-1123
[38] Filipiak J, Kopycki C, Solarz L, Ostrowski J (1998) The SAW Acceleration Sensor. Proceedings European Frequency and Time Forum j.I :229-232.

[39] Filipiak J, Kopycki C, Solarz L, Ostrowski J (1997) Lithium niobiate as the substratum for the SAW acceleration sensor. Proceedings SPIE, The International Society for Optical Engineering j. 3179: 256-260.

IntechOpen